Title Page

Ontogeny of Hepatic Sulfotransferases (SULTs) and Prediction of Age-Dependent Fractional Contribution of Sulfation in Acetaminophen Metabolism

Mayur K. Ladumor, Deepak Kumar Bhatt, Andrea Gaedigk, Sheena Sharma, Aarzoo Thakur, Robin E. Pearce, J. Steven Leeder, Michael B. Bolger, Saranjit Singh, and Bhagwat Prasad

Department of Pharmaceutical Analysis, National Institute of Pharmaceutical Education and Research (NIPER), Mohali, Punjab 160062, India (M.K.L., S.Sharma, A.T. and S.Singh)

Department of Pharmaceutics, University of Washington, Seattle, Washington 98195, USA (D.K.B. and B.P.)

Division of Clinical Pharmacology, Toxicology & Therapeutic Innovation, Department of Pediatrics, Children's Mercy Kansas City; and School of Medicine, University of Missouri-Kansas City, Kansas City, Missouri 64110, USA (A.G., R.E.P. and J.S.L.)

Simulations Plus, Inc., Lancaster, California 93534, USA (M.B.B.)

Running title: Age-dependent abundance of SULTs and its implications

Corresponding authors:

1. Bhagwat Prasad, Ph.D., Department of Pharmaceutics, University of Washington, Seattle, WA 98195, USA. Phone: +1-206-221-2295, E-mail: bhagwat@uw.edu
2. Saranjit Singh, Ph.D., Department of Pharmaceutical Analysis, National Institute of Pharmaceutical Education and Research (NIPER), Mohali (S.A.S. Nagar) 160062, Punjab, India. Phone: +91-172-2292031, E-mail: ssingh@niper.ac.in

DMD Fast Forward. Published on May 17, 2019 as DOI: 10.1124/dmd.119.086462
This article has not been copyedited and formatted. The final version may differ from this version.

Number of

Text pages: 41

Tables: 3

Figures: 5

References: 97

Total words

Abstract: 226

Introduction: 791

Discussion: 1610

Abstract

Cytosolic sulfotransferases (SULTs), including SULT1A, SULT1B, SULT1E and SULT2A isoforms, play noteworthy roles in xenobiotic and endobiotic metabolism. We quantified the protein abundance of SULT1A1, SULT1A3, SULT1B1 and SULT2A1 in human liver cytosol samples (n=194) by LC-MS/MS proteomics. The data were analyzed for their association with age, sex, genotype, and ethnicity of the donors. SULT1A1, SULT1B1, and SULT2A1 showed significant age-dependent protein abundance, whereas SULT1A3 was invariable across 0-70 years. The respective mean abundance of SULT1A1, SULT1B1, and SULT2A1 in neonatal samples was 24, 19 and 38% of the adult levels. Interestingly, unlike UDP-glucuronosyltransferases (UGTs) and cytochrome P450 enzymes (CYPs), SULT1A1 and SULT2A1 showed the highest abundance during early childhood (1 to <6 years), which gradually decreased by ~40% in adolescents and adults. SULT1A3 and SULT1B1 abundances were significantly lower in African Americans as compared to Caucasians. Multiple linear regression analysis further confirmed the association of abundance of SULTs with age, ethnicity, and genotype. To demonstrate clinical application of the characteristic SULT ontogeny profiles, we developed and validated a proteomics-informed physiologically based pharmacokinetic (PBPK) model. The latter confirmed the higher fractional contribution of sulfation over glucuronidation in the metabolism of acetaminophen in children. The study thus highlights that ontogeny-based age-dependent fractional contribution (f_m) of individual drug metabolizing enzymes has better potential in prediction of drug-drug interactions and the effect of genetic polymorphisms in the pediatric population.

Introduction

The human cytosolic sulfotransferases (SULTs) are important Phase II drug metabolizing enzymes (DMEs) that catalyze sulfate conjugation by transferring a sulfonate (SO_3) group from 3'-phosphoadenosine-5'-phosphosulphate (PAPS) to the hydroxyl or amino group of xenobiotic or endobiotic substrates. Several SULT isoforms, i.e., SULT1A1, SULT1A3, SULT1B1, SULT1E1 and SULT2A1 play important role in the metabolism of drugs, environmental toxins, and endogenous steroids. For example, SULT1A1 is involved in the biotransformation of acetaminophen, minoxidil, 4-hydroxytamoxifen, oxymorphone, nalbuphine, nalorphine, naltrexone, isoflavones, estradiol and iodothyronines (Coughtrie et al., 1994; Nishiyama et al., 2002; Nowell and Falany, 2006; Kurogi et al., 2014; Marto et al., 2017). Similarly, SULT1A3 is known to metabolize catecholamines, serotonin, salbutamol, ritodrine, and troglitazone (Eisenhofer et al., 1999; Honma et al., 2002; Hui and Liu, 2015; Bairam et al., 2018); SULT1B1 plays role in elimination of iodothyronines, thyroxine, and 1-naphthol (Fujita et al., 1997; Wang et al., 1998; Gamage et al., 2005); SULT1E1 metabolizes raloxifene and estrogens (Falany et al., 1995; Schrag et al., 2004; Falany et al., 2006; Cubitt et al., 2011); while SULT2A1 assists in metabolism of ciprofloxacin, desipramine, metoclopramide, dehydroepiandrosterone (DHEA), several bile acids, and 25-hydroxyvitamin D_3 (Falany et al., 1994; Meloche et al., 2002; Falany et al., 2004; Cook et al., 2009; Nakamura et al., 2009; Senggunprai et al., 2009; Huang et al., 2010; Wong et al., 2018). Because several of these substrates are relevant to children, hence it is important to characterize age-dependent abundances of these enzymes.

Unlike cytochrome P450 enzymes (CYPs), Phase II drug metabolism pathways are not well characterized for age-dependent activity and expression due to the non-availability of probe substrates, specific inhibitors, and antibodies. Recently, we performed selective quantitative proteomics analysis of UGTs in human liver samples from 137 pediatric and 37 adult samples, where we observed distinct patterns of ontogeny for various UGTs (Bhatt et al., 2018a; Bhatt et al., 2018b). For example, UGT2B17 expression was rarely observed in

children age <9 years, while it sharply increased during teenage. We also observed that UGT1A1 and UGT2B15 were the major neonatal UGTs, whereas UGT1A4 and UGT2B7 were the major adult isoforms. These ontogeny data were used by us to explain age-dependent pharmacokinetics (PK) of UGT substrates in children (Bhatt et al., 2018b).

There are some reports in literature, which indicate that SULT activity is higher than those of UGTs in children, and the phenomenon reverses in adults. For example, acetaminophen glucuronide to sulfate metabolite ratio is reported to increase from 0.34 in newborns to 0.75 in children 3-9 years of age, compared to 1.80 in adults (Miller et al., 1976; Behm et al., 2003).

Such non-monotonic development profiles of DMEs pose a challenge for predicting the fractional metabolism (f_m) by individual enzymes for a given population, e.g., children *versus* adults. The parameter, f_m indicates clinical significance of a drug metabolism pathway, i.e., a drug with high f_m for a particular DME can display greater drug-drug interactions (DDIs) and more pronounced in vivo variability due to genetic polymorphism (Salem et al., 2013; Prasad and Unadkat, 2015; Umehara et al., 2017). Because f_m is proportional to the relative abundance of DMEs, different developmental trajectories for individual enzymes may lead to differential f_m with age, eventually resulting in differential metabolic pathways.

Interestingly, several drugs are metabolized by CYPs, UGTs, and SULTs. However, data are sparse on SULT activity in children and the age-dependent abundance of individual SULT isoforms is not well characterized. In the present study, we targeted to fill this important knowledge gap by investigating protein abundance of SULT1A1, SULT1A3, SULT1B1, and SULT2A1 by a robust LC-MS/MS proteomics methodology (Bhatt and Prasad, 2018). In doing so, we made use of cytosolic fractions prepared from the same human livers, for which UGT ontogeny data were reported by us earlier (Bhatt et al., 2018b).

To additionally demonstrate utility of the SULT ontogeny data generated in this study, we developed proteomics-informed PBPK model of acetaminophen for predicting age-dependent metabolic switching in its elimination. In adult human liver, acetaminophen is

mainly metabolized by conjugation through glucuronidation (52-57% by UGT1A1, UGT1A6, UGT1A9, and UGT2B15) with next important role of sulfation (30-44% by SULT1A1, SULT1A3, SULT1E1 and SULT2A1) and minor contribution of oxidation (5-10% by CYP1A2, CYP2C9, CYP2C19, CYP2D6, CYP2E1 and CYP3A4) (Prescott, 1983; Clements et al., 1984; Critchley et al., 1986; Critchley et al., 2005). A PBPK model is reported in the literature to describe acetaminophen PK in children including neonates and infants (Jiang et al., 2013). However, because selective ontogeny data were not available for the UGTs and SULTs, this model was based on few assumptions regarding DME ontogeny. To address this knowledge deficit, we used the ontogeny data of UGTs (Bhatt et al., 2018b), SULTs (described here) and CYPs (unpublished) to develop and validate a refined acetaminophen pediatric PBPK model.

Materials and Methods

Chemicals and reagents

Iodoacetamide (IAA), dithiothreitol (DTT), mass spectrometry (MS) grade trypsin, bovine serum albumin (BSA) and synthetic heavy labeled peptides were purchased from Thermo Fisher Scientific (Rockford, IL, USA). Purified SULT1A1 and SULT2A1 protein standards were procured from Abnova (Walnut, CA, USA). Chloroform, ethyl ether, MS-grade acetonitrile (99.9% purity), methanol (>99.5% purity), formic acid (≥99.5% purity) and ammonium bicarbonate (98% purity) were purchased from Fischer Scientific (Fair Lawn, NJ, USA).

Human liver cytosol samples

194 human liver samples (137 pediatric and 57 adults), a majority of which were previously characterized by our group for abundance of UGTs (Bhatt et al., 2018b), carboxylesterases (Boberg et al., 2017) and aldehyde and alcohol dehydrogenases (Bhatt et al., 2017), were used in this study. A detailed donor demographic information of these samples is reported in the aforementioned studies. Of the 137 pediatric liver samples, 129 were provided by Children's Mercy Kansas City (Kansas City, MO, USA), which were originally procured from various sources including the National Institute of Child Health and Human Development (NICHD) Brain and Tissue Bank for Developmental Disorders at the University of Maryland; Liver Tissue Cell Distribution System at the University of Minnesota; University of Pittsburgh; Vitron (Tucson, AZ, USA), and XenoTech LLC (Lenexa, KS, USA). The remaining 8 pediatric and 57 adult human liver samples were obtained from the University of Washington School of Pharmacy liver bank. The use of these samples was approved and determined as non-human subject research by the institutional review boards of the Children's Mercy Kansas City (Kansas City, MO, USA) and the University of Washington (Seattle, WA, USA). Information regarding the procurement and storage of these liver samples is described in previous reports (Prasad et al., 2016; Shirasaka et al., 2016; Boberg et al., 2017). The

DMD Fast Forward. Published on May 17, 2019 as DOI: 10.1124/dmd.119.086462
This article has not been copyedited and formatted. The final version may differ from this version.

samples were categorized into following groups based on age, sex and ethnicity: i) *Age*: neonatal (0 to 27 days; n=4), infancy (28 to 364 days; n=17), toddler/early childhood (1 to <6 years; n=30), middle childhood (6 to <12 years; n=38), adolescence (12 to 18 years; n=48) and adulthood (>18 years; n=57); ii) *Sex*: male (n=116), female (n=76) and unknown (n=2); and iii) *Ethnicity*: Caucasian (n=123), African-American (n=29), Hispanic (n=4), Native American (n=1), Pacific Islander (n=1), Asian (n=1), and unknown (n=35).

DNA isolation, genotype and copy number variation (CNV) analysis

Genomic DNA was isolated from liver tissues according to established protocols. Genotyping was performed using PGRN-SeqV1 (Gordon et al., 2016) or the DMET Plus Array, as stated in the manufacturer's protocol (Affymetrix, Santa Clara, CA, USA). *SULT* gene copy number variation was determined using a quantitative multiplex PCR assay described previously (Gaedigk et al., 2012) for the samples provided by the Children's Mercy Kansas City (Kansas City, MO, USA).

Protein extraction, trypsin digestion, and sample preparation

Human liver cytosol (HLC) fractions were isolated from liver tissues by differential centrifugation, employing a previously described method (Pearce et al., 2016). Total cytosolic protein concentration was determined using the bicinchoninic acid (BCA) protein assay kit. Three HLC aliquots (~2 mg/mL) were prepared, separately digested, processed and analyzed by LC-MS/MS using a previously reported protocol (Bhatt et al., 2017), which is detailed in supplementary file. Surrogate peptides of SULT proteins were selected according to an optimized approach (Vrana et al., 2017).

LC-MS/MS instrument and quantitative analysis

LC-MS system consisted of an Acquity UPLC (Waters Technologies, Milford, MA) coupled to Sciex Triple Quadrupole 6500 MS system (Framingham, MA). The mass spectrometer was operated in multiple reaction monitoring (MRM) mode using positive ion electrospray

DMD Fast Forward. Published on May 17, 2019 as DOI: 10.1124/dmd.119.086462
This article has not been copyedited and formatted. The final version may differ from this version.

ionization for targeted peptide analysis. Peak integration and quantification were performed using Skyline software (University of Washington).

The peptides were separated employing Waters Acquity UPLC column (HSS T3, 100 x 2.1 mm, 1.8 µm). The mobile phase was run in a gradient mode, composition of which is described in Supplementary Table 1S. Optimized mass instrument parameters for analysis of surrogate peptides of SULTs, along with information on peptide sequences, and their types, are given in Supplementary Table 2S. Data analysis was performed using a three-step normalization process (Bhatt and Prasad, 2018) to ensure technical robustness. The absolute abundance of SULT1A1 and SULT2A1 was determined by using commercially available purified protein standards as calibrators. However, due to non-availability of protein standards of SULT1A3 and SULT1B1, their quantification was relative, which was done by normalization to total protein.

Statistical analysis of LC-MS/MS proteomics data

The distribution of age, ethnicity and sex-dependent protein expression data were subjected to normal distribution tests (Kolmogorov-Smirnov and Shapiro-Wilk) employing GraphPad Prism 5 software (San Diego, CA). Because the data for all studied proteins were not normally distributed, non-parametric tests were applied for the statistical analysis. For age- and genotype-dependent protein abundance data, analyses were performed using Kruskal-Wallis test followed by Dunn's multiple comparison test. The effect of sex- and ethnicity-dependent protein abundance was evaluated using the Mann-Whitney rank order U-test (using GraphPad Prism software), considering p-values of <0.05 as statistically significant. Jonckheere-Terpstra (JT) test was used for the trend analysis, whereas principal component analysis (PCA) was used to evaluate robustness of sample handling and storage, and also to identify unique patterns in protein abundances, as was done in our earlier studies (Bhatt and Prasad, 2018). Multiple linear regression was performed to rule out confounding effects of multiple covariates (e.g., age *versus* ethnicity) during data analysis. Protein-protein correlation of the studied SULT isoforms was analysed by Spearman correlation. RStudio

(version 1.0.136) was used for JT (*clinfun* package*; jonckheere.test* function), PCA (*prcomp* function and *ggbiplot* package; *ggbiplot* function*)*, multiple linear regression (*lm* function), and Spearman correlation (*PerformanceAnalytics* package*;* chart.Correlation function) analysis. Wherever applicable, a nonlinear allosteric sigmoidal equation 1 was used to fit the ontogeny data (Bhatt et al., 2018b), as age and enzyme abundance relationship was not expected to be linear.

$$A = A_{birth} + \frac{(A_{max} - A_{birth})}{\left(Age_{50}^{h} + X^{h}\right)} \times X^{h} \quad (1)$$

where A is the enzyme abundance at age X; A_{birth} is the enzyme abundance at birth; A_{max} is the maximum average enzyme abundance; Age_{50} is the age in years at which 50% enzyme abundance is reached; X is age in years; and h is Hill coefficient.

Acetaminophen PBPK model development and validation in adults

Acetaminophen PK data in the literature were available mostly either as concentration-time graphs or in the form of tables. The data from plasma concentration-time profiles were extracted using GetData Graph Digitizer (http://www.getdata-graph-digitizer.com/index.php). Additional information, i.e., route of administration, dose strength, dosing regimen and demographic details such as age and weight, was also collected. Whole-body PBPK model of acetaminophen for the adult population was developed using GastroPlus™. For the purpose, reported values of adult plasma clearance after intravenous administration (CL_{IV}) and steady-state volume of distribution (V_{ss}) from existing PBPK model, were used (Jiang et al., 2013). For adult physiology data, the Population Estimates for Age Related (PEAR) physiology module of GastroPlus™ was used and parameters were listed considering the standard population, i.e., healthy male, Caucasian, aged 30 years and 70 kg body weight. Additionally, in vitro experimental enzyme kinetic, biochemical, and physicochemical data were collated from peer-reviewed articles (Chen et al., 1998; Mutlib et al., 2006; Adjei et al., 2008; Laine et al., 2009; Jiang et al., 2013; Villiger et al., 2016; Zurlinden and Reisfeld, 2016). The same are listed in Supplementary Table 3S. The tissue partition coefficients (Kp)

DMD Fast Forward. Published on May 17, 2019 as DOI: 10.1124/dmd.119.086462
This article has not been copyedited and formatted. The final version may differ from this version.

were estimated using the default Lukacova method embedded in the PBPKPlus™ module, considering all organs as perfusion limited tissues (Supplementary Table 3S).

In vivo unbound total intrinsic hepatic clearance of acetaminophen ($CLu_{int,H}$, L/h) was back calculated using the well-stirred model (Yang et al., 2007) as mentioned in equation 2.

$$\mathrm{CLu_{int,H}} = \frac{\mathrm{Q_{H,B}} \times \mathrm{CL_H}}{\mathrm{fu_p} \times \left(\mathrm{Q_{H,B}} - \mathrm{CL_H/B{:}P}\right)} \quad (2)$$

The observed hepatic plasma clearance (CL_H, 18.58 L/h) was obtained from CL_{iv} (19.7 L/h) after subtracting renal plasma clearance (CL_R, 1.12 L/h). It considered the hepatic blood flow ($Q_{H,B}$) as default GastroPlus™ value of 84.36 L/h for 70 kg body weight, unbound fraction in plasma (fu_p) as 0.82 and blood to plasma drug concentration ratio (B:P) as 1.58 (Supplementary Table 3S).

Individual DME isoform mediated clearance (CLu_{int,DME_j} in L/h) was calculated from equation 3 using fraction acetaminophen metabolized by individual DME isoform (f_{m,DME_j}, such as f_{m,UGT_j}, $f_{m,SULT_j}$, f_{m,CYP_j}), fraction of drug cleared through hepatic metabolism ($f_{CL,metabolsim,H} = 1 - f_{CL,renal}$) and $CLu_{int,H}$ values (Supplementary Table 3S). $f_{CL,renal}$ is the unchanged renally cleared fraction of drug.

$$\mathrm{CLu_{int,DME_j}} = \frac{\mathrm{f_{m,DME_j}} \times \ \mathrm{CLu_{int,H}}}{1 - \mathrm{f_{CL,renal}}} \quad (3)$$

In vitro $\mathrm{CL_{int,DME_j}}$ was back calculated based on $\mathrm{CLu_{int,DME_j}}$, using equation 4.

$$\text{In vitro } \mathrm{CL_{int,DME_j}} = \frac{\mathrm{CLu_{int,DME_j}}}{\text{MPPGL or CPPGL} \times \text{Liver weight} \times 60 \times 10^{-6}} \quad (4)$$

where MPPGL is mg microsomal protein per gram adult liver weight (default GastroPlus™ value of 38), CPPGL is mg cytosolic protein per gram of adult liver weight (default GastroPlus™ value of 80), liver weight is in grams (default GastroPlus™ value of 1637.7) and a factor of 60×10^{-6} is for unit conversions.

DMD Fast Forward. Published on May 17, 2019 as DOI: 10.1124/dmd.119.086462
This article has not been copyedited and formatted. The final version may differ from this version.

Thereafter, $V_{max,\,DME_j}$ (pmol/min/mg protein) for individual DME isoforms (i.e., UGT1A1, UGT1A9, UGT2B15, SULT1A1, SULT1A3, SULT1E1, SULT2A1, CYP1A2, CYP2C9, CYP2C19, CYP2D6, CYP2E1 and CYP3A4) were calculated as product of the in vitro K_{m,DME_j} (µM), unbound fraction in microsomes (fu_{mic}) (default GastroPlus™ value of 1) and in vitro CL_{int,DME_j} (µL/min/mg protein) (values in Supplementary Table 3S), using equations 5.

$$V_{max,DME_j} = \text{In vitro } CL_{int,DME_j} \times K_{m,DME_j} \times fu_{mic} \quad (5)$$

The model was applied to simulate the PK profile of various intravenous (IV) dosing regimens of acetaminophen. After qualifying disposition model across different clinical data sets, absorption model was established by integrating oral absorption parameters, such as permeability, solubility, diffusion coefficient, particle size, etc. using “Human-Fasted” gut physiology model of GastroPlus™. Based on literature, the role of intestinal metabolism of acetaminophen was considered negligible (Clements et al., 1984). Similarly, oral PBPK models of acetaminophen were qualified using available clinical data for different dosing regimens, i.e., oral doses of 500-2000 mg.

The predictive performance of the developed models was evaluated by comparing the simulated exposure parameters with literature-based clinical data, in accordance with the criteria suggested in the literature for comparison of AUC and C_{max} (Abduljalil et al., 2014; Huang et al., 2017). The following criteria were considered: i) bioequivalence criteria, wherein the simulated AUC and C_{max} were required to be within 1.25-fold of the observed clinical data; ii) 2-fold criteria, which allows for a 0.5 to 2-fold variability between simulated and observed data, and iii) population-based criteria, wherein the fold change boundary is based on corresponding observed values. In the latter, acceptance criteria were calculated with consideration of sample size (N) and coefficient of variation (%CV) (reported studies lacking N and %CV were excluded). The acceptance ranges of the mean C_{max} and AUC were calculated by the equations 6-8 (Abduljalil et al., 2014; Huang et al., 2017).

$$\sigma = \sqrt{\ln\left[\left(\frac{CV\%}{100}\right)^2 + 1\right]} \quad (6)$$

DMD Fast Forward. Published on May 17, 2019 as DOI: 10.1124/dmd.119.086462
This article has not been copyedited and formatted. The final version may differ from this version.

$$A\bar{x} = \exp\left[\ln(\bar{x}) + 4.26\frac{\sigma}{\sqrt{N}}\right] \quad (7)$$

$$B\bar{x} = \exp\left[\ln(\bar{x}) - 4.26\frac{\sigma}{\sqrt{N}}\right] \quad (8)$$

wherein A and B are the upper and lower boundary limits for simulated data, respectively; $\bar{x}$ is the mean of C_{max} or AUC of acetaminophen, and σ is the standard deviation calculated from the %CV of the C_{max} or AUC.

Once the PBPK model for parent drug was validated, acetaminophen metabolite PK models were developed using parameters described in Supplementary Tables 4S and 5S. Because mechanistic elimination parameters (e.g., active efflux clearance) were not available for the metabolites, we assumed that the metabolites were eliminated unchanged in urine and the metabolite kinetics was formation-rate limited. Accordingly, the predicted total amount of metabolites eliminated in urine (A_e) was compared with the observed data.

Development of pediatric acetaminophen PBPK model

Following the development of adult acetaminophen PBPK model, we integrated ontogeny data (mean and 95% confidence interval of protein abundance) of SULTs (from this study), UGTs (Bhatt et al., 2018b), and CYPs (unpublished) with pediatric physiological parameters determined from the PEAR physiology module of GastroPlus™ software. The intention was to predict acetaminophen PK profile in the pediatric population. Besides major SULTs quantified in this study, published data of SULT1E1 (Duanmu et al., 2006) were also utilized for the model development. The pediatric population models were built for five age groups representing the mean of neonates (14 days and 3.7 kg body weight); infants (6 months and 8.23 kg body weight), early childhood (4 years and 17.34 kg body weight), middle childhood (9 years and 34.45 kg body weight) and adolescents (15 years and 63.69 kg body weight). Further, based on the availability of clinical data, we also simulated data for three additional age-groups, infants (1 year and 10.23 kg body weight), children (7 years and 26.54 kg body weight) and adolescents (14 years and 58.74 kg body weight). V_{ss} was estimated based on approach explained in Supplementary Table 3S. The fu_p was adjusted by the software to

DMD Fast Forward. Published on May 17, 2019 as DOI: 10.1124/dmd.119.086462
This article has not been copyedited and formatted. The final version may differ from this version.

account for both, age related differences in plasma protein level as well as binding to plasma lipids.

Although similar protein abundance values were considered for adult and pediatric samples by the software, but to address the enzyme ontogeny, we adjusted V_{max,DME_j} (pmol/min/mg protein) values for individual enzymes based on age-dependent protein abundances of SULTs, UGTs and CYPs (Supplementary Table 3S) using equation 9 and used then as an input in the Enzymes and Transporter module of GastroPlus™.

$$\text{Adjusted } V_{max,DME_j} = V_{max,DME_j} \times SF_{DME_j} \times SF_{\text{MPPGL or CPPGL}} \quad (9)$$

where, scale factor (SF) was generated for calculating the age-dependent abundance of three DME isoforms and MPPGL using equations 10 and 11, respectively. The resultant data is listed in Supplementary Table 6S.

$$SF_{DME_j} = \frac{\text{Mean or 95 \%CI abundance of DME in pediatric population}}{\text{Mean abundance of DME in healthy adults}} \quad (10)$$

$$SF_{MPPGL} = \frac{\text{Mean MPPGL}_{\text{pediatric}}}{\text{Mean MPPGL}_{\text{adult}}} \quad (11)$$

Thus, age-dependent MPPGL values were integrated for CYPs and UGTs (Calvier et al., 2018). However, CPPGL value was considered similar for adults and pediatrics as it was observed to be age-independent (unpublished data).

Further, scaled CLu_{int,DME_j} value was obtained through in vitro-in vivo extrapolation (IVIVE) using equation 12.

$$\text{Scaled } CLu_{int,DME_j} = \frac{\text{Adjusted } V_{max,DME_j}}{K_{m,DME_j} \times fu_{mic}} \times \text{MPPGL or CPPGL} \times \text{Liver weight} \times 60 \times 10^{-6} \quad (12)$$

Default GastroPlus™ liver weight values for each age group were input in the above mentioned equation, which account for the age dependent change, viz., neonatal (123.44 g at 14 days); infancy (228.01 g at 6 months), infancy (325.11 g at 1 year), early childhood

DMD Fast Forward. Published on May 17, 2019 as DOI: 10.1124/dmd.119.086462
This article has not been copyedited and formatted. The final version may differ from this version.

(592.12 g at 4 years), children (726.23 g at 7 years), middle childhood (906.24 g at 9 years), adolescence (1391.9 g at 14 years) and adolescence (1482.7 g at 15 years).

Age-dependent $f_{m,\ DME_j}$ value was obtained from drug-drug interaction (DDI) module of GastroPlus™ as well as from scaled CLu_{int,DME_j} value as per equation 13.

$$f_{m,DME_j} = \frac{\text{Scaled } CLu_{int,DME_j}}{\sum \text{Scaled } CLu_{int,DME_j}} \times (1 - f_{CL,renal}) \quad (13)$$

Since fraction of drug cleared unchanged renally ($f_{CL,renal}$ or f_e) is age-independent (Miller et al., 1976), $f_{CL,renal}$ value was considered to be constant (~0.057) among all the age groups (Supplementary Table 3S).

Cumulative $f_{m,SULT}$, $f_{m,UGT}$ and $f_{m,CYP}$ values were derived from total of individual isoforms of SULT, UGT and CYP, respectively, using equation 14.

$$f_{m,SULT/UGT/CYP} = \sum f_{m,SULT_j/UGT_j/CYP_j} \quad (14)$$

The scaled model was then used to predict acetaminophen PK in children and the predictions were compared with the reported observed data. The model was further extended to predict the dosing regimen in neonates and infants, which was qualified by comparison with the dose adjustments recommended by the FDA. Validation of the pediatric model was done by application of the same approach, as discussed for the adult model. Also similar to the adults, prediction of A_e of the metabolites and unchanged drug was done in case of the pediatric groups.

Results

Abundance and variability of human SULT enzymes

The mean cytosolic protein abundances of SULT1A1, SULT1A3, SULT1B1 and SULT2A1 in the neonates (0 to 27 days) were 24, 47, 19, and 38%, respectively, of the mean values for the adults (>18 years) (Table 1 and Figure 1). In the infants (28 to 364 days), the values for these SULT isoforms were 80, 76, 41, and 111% of the adult levels, respectively. SULT1A1 protein abundance in early childhood (1 to <6 years) was ~7-fold higher compared to the neonates and ~2-fold higher than the adults. The association of categorical SULT1A3 abundance data with age was not significant (Figure 1). SULT1B1 protein abundance in the adults was found to be ~5.4 and 2.4 fold higher than the neonates (p-value <0.05) and the infants (p-value <0.0001), respectively. Similarly, SULT2A1 protein abundance in early childhood was ~4 and ~2-folds higher as compared to the neonates and adolescents (12 to 18 years), respectively.

The developmental trajectory of each SULT isoform was also assessed using age as a continuous variable (Supplementary Figure 1S). Data for both SULT1A3 and SULT1B1 could be adequately characterized by a nonlinear allosteric sigmoidal model, justified by the fact that age and enzyme abundance relationship was not linear. The latter is consistent with the literature on ontogeny of DMEs (Johnson et al., 2006; Upreti and Wahlstrom, 2016; Boberg et al., 2017; Emoto et al., 2018). In both cases, the age_{50} value (the age at which protein expression reached 50% of the maximum adult abundance) was determined to be 0.91 years, i.e., ~11 months (Supplementary Figure 1S and Supplementary Table 7S). The high biological variability in SULT1A3 and SULT1B1 resulted in poor confidence in the age_{50} calculation, yet age-dependent abundance of these enzymes was supported by other statistical methods (Kruskal-Wallis test, multiple linear regression analysis, and JT trend analysis). However, this ontogeny model and statistical tests were not appropriate for SULT1A1 and SULT2A1 data, in which the developmental trajectories were characterized by

protein abundance reaching maximum values in the toddler/early childhood group, and subsequently declining to the adult values.

Association of ethnicity, single nucleotide polymorphisms (SNPs), copy number variations (CNVs) and sex with SULT abundance

The protein abundance of SULT1A3 and SULT1B1 was significantly higher in Caucasians as compared to African-Americans (p-value <0.0001) (Table 1 and Figure 2). But age-ethnicity interplay made it difficult to draw a precise conclusion in the first instance. Therefore, multiple linear regression analysis was relied upon, as it considered effect of age *versus* ethnicity independently. Based on the results, it could be concluded that ethnicity was indeed one of the key covariate in the abundance of SULT1A3 and SULT1B1. Additionally, Mann-Whitney test for association of ethnicity with age groups <12 and ≥12 years also supported the conclusion drawn by the multiple linear regression analysis. A significant association (trend analysis; JT test) of SULT1B1 protein abundance with SNP rs11249460 (TT<CT<CC) was also observed. Detailed data analyses in this context are provided in Supplementary Tables 8S-9S and Figures 2S-3S.

Also, trend (JT test) and multiple linear regression analyses confirmed significantly (p-value = 0.042) higher median SULT1A1 abundance with increasing copy number (CN1 to CN4). No test revealed any relationship with ethnicity and sex in this case. The Mann-Whitney test indicated no association of ethnicity and SULT2A1 abundance, perhaps because of age-related variability. On the other hand, multiple linear regression analysis concluded that ethnicity was one of the key variables in the abundance of SULT2A1. Interestingly, the multiple linear regression analysis showed a modest, but significantly higher abundance of SULT2A1 in females than in males (p-value <0.05). No significant association of protein abundance was observed for other high frequency SNPs, i.e., rs982861 (SULT1A1); rs11569731, rs11731028, rs11731028, rs1604741 (SULT1B1) and rs296365 (SULT2A1).

DMD Fast Forward. Published on May 17, 2019 as DOI: 10.1124/dmd.119.086462
This article has not been copyedited and formatted. The final version may differ from this version.

The statistical results for this portion are summarized in Supplementary Tables 8S-9S and Figures 4S-5S.

Protein-protein correlation

This study, which was done with an objective to look for co-regulation of SULT proteins, highlighted strong correlation between abundance levels of SULT1A1 and SULT2A1 (r^2 = 0.60, p-value <0.001; Supplementary Figure 6S). Similarly, SULT1A3 showed correlation with SULT1B1 (r^2 = 0.61 and p-value <0.05).

PCA analysis of proteomics data

The PCA analysis, which was done to evaluate robustness of sample handling and storage, and to identify unique patterns in protein abundances, highlighted that there was no degradation of samples before and during processing. As shown in our previous report (Bhatt and Prasad, 2018), data for degraded samples clustered distinctly towards the left lower side of PC1 *versus* PC2 plots. In the present case, there was no clustering in the indicated region (Supplementary Figure 7S), suggesting that our sample quality was not compromised overall.

Regarding identification of unique patterns, the circled areas in PCA plot (Supplementary Figure 7S) confirmed higher variability in the pediatric groups (0-18 years) for all SULT enzymes, as compared to the adults.

Prediction of age-dependent fractional contribution (f_m) of sulfation over glucuronidation in acetaminophen metabolism

Considering demonstration of the application of the ontogeny data as key objective of this study, other population covariates were not considered for overall interindividual variability prediction (%CI), meaning that the predictions were made solely based on mean and 95 %CI data of protein abundance. As shown in Table 2 and Figures 3 and 4, the observed *versus* predicted AUC and C_{max} values of acetaminophen for both IV and oral administration in

fasted- and fed-states were within the acceptance criteria. It is clearly evident from data in Table 2 that 2-fold and population based criteria yielded higher number of results within acceptable limits than the bioequivalence criterion. This confirmed that the latter was stringent in comparison, a reason due to which it is rarely used in PBPK modeling. Hence, our results relied only on 2-fold and population based criteria. Although, 2-fold criterion is most commonly used for PBPK model validation, hence it was considered as the reference criterion for model acceptance in this study. But as it is also an arbitrary method and does not consider biological variability in the data, additional analysis of predictive performance of PBPK model was done using the population based criterion.

The validated adult PBPK model was employed for prediction of PK in pediatric population considering all relevant information gathered. There was under-prediction of acetaminophen AUC for the pediatric population, when DME ontogeny data were not considered (Figure 4). The ontogeny-based model predicted $f_{m,\,ratio}$ values (e.g., $f_{m,UGT}/f_{m,SULT}$) were 0.46, 0.56, and 1.71 in neonates, children and adults, respectively (Table 3 and Figure 5). These predicted f_m and corresponding A_e data were in agreement with those observed (Figure 5). Data in Supplementary Table 10S show that model predicted pediatric PK data even correlated well with the FDA recommended dose adjustments.

Discussion

Some data exist in the literature regarding the ontogeny of SULT1A1, SULT1A3, SULT2A1 and SULT1E1 (Brashear et al., 1988; Barker et al., 1994; Richard et al., 2001; Behm et al., 2003; Pacifici, 2005; Stanley et al., 2005; Duanmu et al., 2006; Ekström and Rane, 2015). However, several limitations are associated with these studies, like: i) lack of specific antibodies used for the Western blotting, ii) use of non-selective in vitro or in vivo probe substrates for the activity, iii) sparse and smaller number of samples, and iv) inconsistent mRNA data that show poor correlation with functional activity. Hence, a comprehensive investigation on ontogeny of SULT enzymes using LC-MS/MS proteomics approach was performed in this study.

Amongst the notable findings, we observed that the ontogeny of hepatic SULTs are opposite to the trend of ontogeny of UGTs and most CYPs that are poorly expressed in fetal and early neonatal ages but are abundant in adult (Pacifici et al., 1982; Choonara et al., 1989; Pacifici et al., 1993; McCarver and Hines, 2002; Hines, 2007; Upreti and Wahlstrom, 2016). Using the same donor samples, we recently reported that, as compared to the adults, levels of UGTs were 3 to 40% in the neonates, 24 to 60% in the infants, and 37 to 72% in the childhood age (Bhatt et al., 2018b). These data are consistent with the literature, where the adult to the fetal ratios of UGT and SULT activities are shown to be 114 and 3.5, respectively (Pacifici et al., 1989). Similarly, SULT1A3 mediated dopamine sulfation activity is shown to be 3-fold higher in the fetal liver as compared to the adult liver, whereas an opposite trend was observed in SULT1A1 4-nitrophenol sulfation activity (Cappiello et al., 1991). Ritodrine, a tocolytic agent for the management of preterm labor, is inactivated by sulfation and glucuronidation. The ratio of ritodrine sulfate to glucuronide in urine was found to be higher in newborns, whereas the ratio was equal in maternal urine (Brashear et al., 1988; Pacifici et al., 1993). Such observed differential DME ontogeny has a direct in vivo significance for drugs metabolized by multiple DMEs (e.g., SULTs, UGTs, CYPs, etc.).

Our data do not agree with the reported ones on few occasions. For example, we observed that SULTs (particularly, SULT1A1 and SULT2A1) are expressed higher in childhood age (1-12 years) as compared to the adolescents and adults. It is in difference to the observations by Duanmu et al. who found no difference in hepatic SULT1A1 and SULT2A1 abundance in postnatal samples (Duanmu et al., 2006). A limited number of pediatric samples from children between 2-10 years could be a potential reason for this discrepancy. Similarly, although SULT1A3 was detected in all age groups in our study, this enzyme was only detected in fetal and neonatal livers by others (Richard et al., 2001). It indicates better sensitivity of our method. Further, LC-MS/MS proteomics allowed discrimination of the highly homologous SULT proteins as compared to conventional antibody- or activity-based methods.

Practically nothing is previously known regarding SULT1B1 ontogeny. Our data show a significant and gradual age-dependent increase in SULT1B1 abundance during the first year of life, unlike SULT1A1 and SULT2A1 enzymes, but the behavior was similar to CYPs and UGTs.

The mechanisms that regulate the age-dependent abundance of SULTs remain unclear. However, transcription and environmental factors could be the potential regulators of SULT expression during development. The differential tissue and cross-species expression are considered to be regulated by aryl hydrocarbon receptor (AhR), constitutive androstane receptor (CAR), pregnane X receptor (PXR), liver X receptor (LXR), farnesoid X receptor (FXR), peroxisome proliferator-activated receptors (PPARs), and vitamin D receptor (VDR) (Dubaisi et al., 2018). As the expression of some of these transcriptional factors, e.g., PXR, PPARα or PPARγ, is age-dependent (Balasubramaniyan et al., 2005), one can anticipate their role in corresponding developmental change in SULT abundance. In particular, the expression of SULT2A1 is reported to increase 2-fold in fetal hepatocyte culture by agonists of PPARα (GW7647) or PPARγ (rosiglitazone) and suppressed by the FXR agonist (GW4064) (Dubaisi et al., 2018). Steroidogenic factor 1 (SF1) and GATA-binding factor 6

(GATA6) are also reported to be involved in regulation of SULT2A1 in adrenal (Saner et al., 2005). Similarly, because SULT2A1 is the major DHEA metabolizing enzyme and the levels of urinary DHEA and hydroxylated DHEA (representing sulfate conjugates) transforms during early to late childhood age, one can postulate that DHEA is involved in the regulation of SULT2A1 during the pubertal development (Rainey et al., 2002; Remer et al., 2005). This is also supported by the fact that adrenal expression of SULT2A1 increases with the gradual growth of adrenal zona reticularis (ZR) (Nakamura et al., 2009).

In accordance with our objective, we applied the differential ontogeny data of SULTs, UGTs and CYPs to estimate the effect of age on f_m values of these enzymes in acetaminophen metabolism. The major reason to select this drug was the availability of extensive reported in vitro and PK data in the neonates, infants and children (CDER, 2010; CDER, 2015). The predicted f_m and corresponding metabolite A_e data were in good agreement with the observed data (Figure 5). For example, the ratio of UGT/SULT f_m for acetaminophen was simulated to be 0.46, 0.56, and 1.71 as compared to the observed value of fraction excreted of glucuronide/sulfate of 0.34, 0.75, and 1.8 in the neonates, children, and adults, respectively (Miller et al., 1976). Acetaminophen is also transformed to *N*-acetyl-*p*-benzoquinone imine (NAPQI), a hepatotoxic metabolite mainly formed through oxidative mechanism via CYP2E1. Accurate f_m prediction for CYP mediated bio-activation of acetaminophen is important for predicting toxicity in children. With higher contribution of SULT in the clearance of various drugs in children, including acetaminophen, it is hypothesized that SULT-mediated DDIs or food-drug interactions, may be significant in pediatric population.

Our proteomics-informed PBPK predictions of acetaminophen PK in neonates and infants are consistent with the FDA label doses for acetaminophen injection. For example, FDA suggests a dose reduction of 50% and 33% for the neonates and infants, respectively, to produce PK exposure similar to the children. The origin of this dose reduction is related to age-dependent in vivo clearance of the drug (Zuppa et al., 2011). The extent of

acetaminophen dose reduction in pediatrics is reasonably captured by our model (Supplementary Table 10S).

No significant association of ethnicity has been previously reported for sulfation clearance of acetaminophen in adults (African Americans and European Americans) (Court et al., 2017). We rather found that SULT1A3 and SULT1B1 abundances were significantly lower in African Americans as compared to Caucasians, which represented majority of pediatric samples. Although the mechanisms leading to these differences are unknown, genetic polymorphisms or environmental factors could be tested in the future as the potential contributors.

No association of sex with enzyme abundance was observed across all age groups and ethnicity for SULT1A1, SULT1A3 and SULT1B1, albeit multiple linear regression analysis showed a modest, but significantly higher abundance of SULT2A1 in the females consistent with the reported mouse data (Kocarek et al., 2008) and perhaps due to role of SULT2A1 in androgen disposition.

Drugs such as clomiphene, danazol, imipramine, chlorpheniramine, spironolactone, chlorpromazine, amitryptiline, and propranolol are potent inhibitors of SULT enzymes (Coughtrie et al., 1994; Marto et al., 2017), which can produce greater DDIs with SULT substrates in children. A risk of SULT mediated drug-food interactions also exists in children (Nishimuta et al., 2007), as constituents of certain beverages can inhibit SULT enzymes. Various endogenous molecules, such as bile acid, estrogen, thyroid hormones, catecholamines, DHEA, etc., can be differentially affected by modulators of SULT activity, depending on the age (Coughtrie et al., 1994; Coughtrie, 2002). The ontogeny data of SULTs presented here can prove useful in interpreting these data.

Regarding limitations of this study, we were unable to quantify SULT1E1 due to a higher limit of quantification of its surrogate peptide. Further, data for SULT2A1 CNVs and SNPs including rs296361, which have previously been shown to affect protein abundance (Ekström and Rane, 2015; Wong et al., 2018), were not available for all the samples. Nevertheless, our large sample size precludes potential confounding effect of the genetic

variability on the conclusions regarding the ontogeny. Although we have not reported any activity data in this study, we recently showed that SULT2A1 activity correlated well with the abundance data quantified by the same LC-MS/MS method (Wong et al., 2018). The absolute levels of SULT1A1 and SULT2A1 were quantified using the commercially available purified protein standards, however, no further purification and characterization of these standards were conducted and the purity was assumed to be >95%. Further, the PBPK model accurately predicted AUC as well as C_{max} and T_{max} for IV dosing. However, the predicted values of C_{max} and T_{max} for oral dosing were not accurate. This may be explained by a highly variable absorption rate of acetaminophen, which is affected by food and formulation type, including excipients (e.g., sodium bicarbonate) (Rostami-Hodjegan et al., 2002). In the fed-state, where the gastric emptying time is ~1 hour, as compared to 15 min for the fasting state, significantly decreased C_{max} and delayed T_{max} were predicted (Figure 3). In summary, in this first comprehensive report of its kind, we successfully established ontogeny of SULT1A1, SULT1A3, SULT1B1 and SULT2A1 enzymes in a large group of donor human livers (n=194) using quantitative LC-MS/MS proteomics approach. This study is a typical case of pediatric drug metabolism prediction, in situations when multiple metabolic Phase I and Phase II pathways are involved. The ontogeny data were applied to predict age-dependent f_m values for DMEs (SULTs, UGTs, and CYPs) involved in acetaminophen metabolism. The age-dependent f_m data can be further applied to predict DDIs, drug-food interactions and for the predicting variability caused by genetic variation.

Acknowledgments

The authors thank Mr Aravind Rachapally, Mr Sarang Mishra and Ms Priyanka Bobe for assisting in PBPK modeling and simulation. We thank Simulations Plus (Lancaster, CA, USA) for providing license access to GastroPlus™ v9.6 software.

Authorship contributions

Participated in research design: M.K.L, D.K.B., J.S.L., S.Singh, B.P.

Conducted experiments: M.K.L, D.K.B., A.G., R.E.P., S.Sharma, A.T., B.P.

Performed data analysis: M.K.L, D.K.B, A.G., S.Sharma, A.T., M.B.B., B.P.

Wrote or contributed to the writing of the manuscript: M.K.L, D.K.B., A.G., S.Sharma, A.T., R.E.P., J.S.L., M.B.B., S.Singh, B.P.

References

Abduljalil K, Cain T, Humphries H, and Rostami-Hodjegan A (2014) Deciding on success criteria for predictability of pharmacokinetic parameters from in vitro studies: an analysis based on in vivo observations. *Drug Metab Dispos* **42:**1478-1484.

Adjei AA, Gaedigk A, Simon SD, Weinshilboum RM, and Leeder JS (2008) Interindividual variability in acetaminophen sulfation by human fetal liver: implications for pharmacogenetic investigations of drug‐induced birth defects. *Birth Defects Res A Clin Mol Teratol* **82:**155-165.

Alam S, Roberts R, and Fischer L (1977) Age-related differences in salicylamide and acetaminophen conjugation in man. *J Pediatr* **90:**130-135.

Allegaert K, Naulaers G, Vanhaesebrouck S, and Anderson BJ (2013) The paracetamol concentration‐effect relation in neonates. *Paediatr Anaesth* **23:**45-50.

Bairam AF, Rasool MI, Alherz FA, Abunnaja MS, El Daibani AA, Gohal SA, Kurogi K, Sakakibara Y, Suiko M, and Liu M-C (2018) Sulfation of catecholamines and serotonin by SULT1A3 allozymes. *Biochem Pharmacol* **151:**104-113.

Balasubramaniyan N, Shahid M, Suchy FJ, and Ananthanarayanan M (2005) Multiple mechanisms of ontogenic regulation of nuclear receptors during rat liver development. *Am J Physiol Gastrointest Liver Physiol* **288:**G251-G260.

Barker EV, Hume R, Hallas A, and Coughtrie W (1994) Dehydroepiandrosterone sulfotransferase in the developing human fetus: quantitative biochemical and immunological characterization of the hepatic, renal, and adrenal enzymes. *Endocrinology* **134:**982-989.

Behm M, Abdel‐Rahman S, Leeder J, and Kearns G (2003) Ontogeny of phase II enzymes: UGT and SULT. *Clin Pharmacol Ther* **73:**P29-P29.

Bhatt DK, Basit A, Zhang H, Gaedigk A, Lee S-b, Claw KG, Mehrotra A, Chaudhry AS, Pearce RE, and Gaedigk R (2018a) Hepatic abundance and activity of androgen and drug metabolizing enzyme, UGT2B17, are associated with genotype, age, and sex. *Drug Metab Dispos* **46:**888-896.

Bhatt DK, Gaedigk A, Pearce RE, Leeder JS, and Prasad B (2017) Age-dependent protein abundance of cytosolic alcohol and aldehyde dehydrogenases in human liver. *Drug Metab Dispos* **45:**1044-1048.

Bhatt DK, Mehrotra A, Gaedigk A, Chapa R, Basit A, Zhang H, Choudhari P, Boberg M, Pearce RE, and Gaedigk R (2018b) Age‐and genotype‐dependent variability in the protein abundance and activity of six major uridine diphosphate‐glucuronosyltransferases in human liver. *Clin Pharmacol Ther* doi: 10.1002/cpt.1109.

Bhatt DK and Prasad B (2018) Critical issues and optimized practices in quantification of protein abundance level to determine interindividual variability in DMET proteins by LC‐MS/MS proteomics. *Clin Pharmacol Ther* **103:**619-630.

Boberg M, Vrana M, Mehrotra A, Pearce RE, Gaedigk A, Bhatt DK, Leeder JS, and Prasad B (2017) Age-dependent absolute abundance of hepatic carboxylesterases (CES1 and CES2) by LC-MS/MS proteomics: application to PBPK modeling of oseltamivir in vivo pharmacokinetics in infants. *Drug Metab Dispos* **45:**216-223.

Brashear WT, Kuhnert BR, and Wei R (1988) Maternal and neonatal urinary excretion of sulfate and glucuronide ritodrine conjugates. *Clin Pharmacol Ther* **44:**634-641.

Calvier EA, Krekels EH, Yu H, Välitalo PA, Johnson TN, Rostami‐Hodjegan A, Tibboel D, van der Graaf PH, Danhof M, and Knibbe CA (2018) Drugs being eliminated via the same pathway will not always require similar pediatric dose adjustments. *CPT Pharmacometrics Syst Pharmacol* **7:**175-185.

Cappiello M, Giuliani L, Rane A, and Pacifici G (1991) Dopamine sulphotransferase is better developed than p-nitrophenol sulphotransferase in the human fetus. *Dev Pharmacol Ther* **16:**83-88.

CDER (2010) Application number 022450. Clinical Pharmacology and Biopharmaceutics Review(s) https://www.accessdata.fda.gov/drugsatfda_docs/nda/2010/022450Orig1s000ClinPharmR.pdf.

CDER (2015) Application number 204767. Printed Labeling https://www.accessdata.fda.gov/drugsatfda_docs/nda/2015/204767Orig1s000TOC.cfm.

Chen W, Koenigs LL, Thompson SJ, Peter RM, Rettie AE, Trager WF, and Nelson SD (1998) Oxidation of acetaminophen to its toxic quinone imine and nontoxic catechol metabolites by baculovirus-expressed and purified human cytochromes P450 2E1 and 2A6. *Chem Res Toxicol* **11:**295-301.

Choonara I, McKay P, Hain R, and Rane A (1989) Morphine metabolism in children. *Br J Clin Pharmacol* **28:**599-604.

Clements J, Critchley J, and Prescott L (1984) The role of sulphate conjugation in the metabolism and disposition of oral and intravenous paracetamol in man. *Br J Clin Pharmacol* **18:**481-485.

Cook IT, Duniac-Dmuchowski Z, Kocarek TA, Runge-Morris M, and Falany CN (2009) 24-Hydroxycholesterol sulfation by human cytosolic sulfotransferases: formation of monosulfates and disulfates, molecular modeling, sulfatase sensitivity and inhibition of LXR activation. *Drug Metab Dispos* **37:**2069-2078.

Cook SF, Stockmann C, Samiee-Zafarghandy S, King AD, Deutsch N, Williams EF, Wilkins DG, Sherwin CM, and van Den Anker JN (2016) Neonatal maturation of paracetamol (acetaminophen) glucuronidation, sulfation, and oxidation based on a parent-metabolite population pharmacokinetic model. *Clin Pharmacokinet* **55:**1395-1411.

Coughtrie M (2002) Sulfation through the looking glass-recent advances in sulfotransferase research for the curious. *Pharmacogenomics J* **2:**297.

Coughtrie MW, Bamforth KJ, Sharp S, Jones AL, Borthwick EB, Barker EV, Roberts RC, Hume R, and Burchell A (1994) Sulfation of endogenous compounds and xenobiotics-interactions and function in health and disease. *Chem Biol Interact* **92:**247-256.

Court MH, Zhu Z, Masse G, Duan SX, James LP, Harmatz JS, and Greenblatt DJ (2017) Race, gender, and genetic polymorphism contribute to variability in acetaminophen pharmacokinetics, metabolism, and protein-adduct concentrations in healthy African-American and European-American volunteers. *J Pharmacol Exp Ther* **362:**431-440.

Critchley J, Critchley L, Anderson P, and Tomlinson B (2005) Differences in the single‐oral‐dose pharmacokinetics and urinary excretion of paracetamol and its conjugates between Hong Kong Chinese and Caucasian subjects. *J Clin Pharm Ther* **30:**179-184.

Critchley J, Nimmo G, Gregson C, Woolhouse N, and Prescott L (1986) Inter‐subject and ethnic differences in paracetamol metabolism. *Br J Clin Pharmacol* **22:**649-657.

Cubitt HE, Houston JB, and Galetin A (2011) Prediction of human drug clearance by multiple metabolic pathways-integration of hepatic and intestinal microsomal and cytosolic data. *Drug Metab Dispos* **39:**864-873.

Duanmu Z, Weckle A, Koukouritaki SB, Hines RN, Falany JL, Falany CN, Kocarek TA, and Runge-Morris M (2006) Developmental expression of aryl, estrogen, and hydroxysteroid sulfotransferases in pre- and postnatal human liver. *J Pharmacol Exp Ther* **316:**1310-1317.

Dubaisi S, Barrett KG, Fang H, Guzman-Lepe J, Soto-Gutierrez A, Kocarek TA, and Runge-Morris M (2018) Regulation of cytosolic sulfotransferases in models of human hepatocyte development. *Drug Metab Dispos* **46:**1146-1156.

Eisenhofer G, Coughtrie MW, and Goldstein DS (1999) Dopamine sulphate: an enigma resolved. *Clin Exp Pharmacol Physiol* **26:**S41-53.

Ekström L and Rane A (2015) Genetic variation, expression and ontogeny of sulfotransferase SULT2A1 in humans. *Pharmacogenomics J* **15:**293.

Emoto C, Johnson TN, Neuhoff S, Hahn D, Vinks AA, and Fukuda T (2018) PBPK model of morphine incorporating developmental changes in hepatic OCT1 and UGT2B7 proteins to explain the variability in clearances in neonates and small infants. *CPT Pharmacometrics Syst Pharmacol* **7:**464-473.

Falany CN, Krasnykh V, and Falany JL (1995) Bacterial expression and characterization of a cDNA for human liver estrogen sulfotransferase. *J Steroid Biochem Mol Biol* **52:**529-539.

Falany CN, Wheeler J, Oh TS, and Falany JL (1994) Steroid sulfation by expressed human cytosolic sulfotransferases. *J Steroid Biochem Mol Biol* **48:**369-375.

Falany JL, Macrina N, and Falany CN (2004) Sulfation of tibolone and tibolone metabolites by expressed human cytosolic sulfotransferases. *J Steroid Biochem Mol Biol* **88:**383-391.

Falany JL, Pilloff DE, Leyh TS, and Falany CN (2006) Sulfation of raloxifene and 4-hydroxytamoxifen by human cytosolic sulfotransferases. *Drug Metab Dispos* **34:**361-368.

Fujita K-i, Nagata K, Ozawa S, Sasano H, and Yamazoe Y (1997) Molecular cloning and characterization of rat ST1B1 and human ST1B2 cDNAs, encoding thyroid hormone sulfotransferases. *J Biochem* **122:**1052-1061.

Gaedigk A, Twist GP, and Leeder JS (2012) CYP2D6, SULT1A1 and UGT2B17 copy number variation: quantitative detection by multiplex PCR. *Pharmacogenomics* **13:**91-111.

Gamage N, Barnett A, Hempel N, Duggleby RG, Windmill KF, Martin JL, and McManus ME (2005) Human sulfotransferases and their role in chemical metabolism. *Toxicol Sci* **90:**5-22.

Gordon A, Fulton RS, Qin X, Mardis ER, Nickerson DA, and Scherer S (2016) PGRNseq: a targeted capture sequencing panel for pharmacogenetic research and implementation. *Pharmacogenet Genomics* **26:**P161-168.

Hines RN (2007) Ontogeny of human hepatic cytochromes P450. *J Biochem Mol Toxicol* **21:**169-175.

Honma W, Shimada M, Sasano H, Ozawa S, Miyata M, Nagata K, Ikeda T, and Yamazoe Y (2002) Phenol sulfotransferase, ST1A3, as the main enzyme catalyzing sulfation of troglitazone in human liver. *Drug Metab Dispos* **30:**944-949.

Huang J, Bathena S, Tong J, Roth M, Hagenbuch B, and Alnouti Y (2010) Kinetic analysis of bile acid sulfation by stably expressed human sulfotransferase 2A1 (SULT2A1). *Xenobiotica* **40:**184-194.

Huang W, Nakano M, Sager JE, Ragueneau-Majlessi I, and Isoherranen N (2017) Physiologically based pharmacokinetic (PBPK) model of the CYP2D6 probe atomoxetine: extrapolation to special populations and drug-drug interactions. *Drug Metab Dispos* **45:**1156-1165.

Hui Y and Liu M-C (2015) Sulfation of ritodrine by the human cytosolic sulfotransferases (SULTs): effects of SULT1A3 genetic polymorphism. *Eur J Pharmacol* **761:**125-129.

Jiang XL, Zhao P, Barrett J, Lesko L, and Schmidt S (2013) Application of physiologically based pharmacokinetic modeling to predict acetaminophen metabolism and pharmacokinetics in children. *CPT Pharmacometrics Syst Pharmacol* **2:**1-9.

Johnson TN, Rostami-Hodjegan A, and Tucker GT (2006) Prediction of the clearance of eleven drugs and associated variability in neonates, infants and children. *Clin Pharmacokinet* **45:**931-956.

Kamali F, Edwards C, and Rawlins M (1992) The effect of pirenzepine on gastric emptying and salivary flow rate: constraints on the use of saliva paracetamol concentrations for the determination of paracetamol pharmacokinetics. *Br J Clin Pharmacol* **33:**309-312.

Kocarek TA, Duanmu Z, Fang H-L, and Runge-Morris M (2008) Age- and sex-dependent expression of multiple murine hepatic hydroxysteroid sulfotransferase (SULT2A) genes. *Biochem Pharmacol* **76:**1036-1046.

Kurogi K, Chepak A, Hanrahan MT, Liu M-Y, Sakakibara Y, Suiko M, and Liu M-C (2014) Sulfation of opioid drugs by human cytosolic sulfotransferases: metabolic labeling study and enzymatic analysis. *Eur J Pharm Sci* **62:**40-48.

Laine J, Auriola S, Pasanen M, and Juvonen R (2009) Acetaminophen bioactivation by human cytochrome P450 enzymes and animal microsomes. *Xenobiotica* **39:**11-21.

Manyike PT, Kharasch ED, Kalhorn TF, and Slattery JT (2000) Contribution of CYP2E1 and CYP3A to acetaminophen reactive metabolite formation. *Clin Pharmacol Ther* **67:**275-282.

Marto N, Morello J, Monteiro EC, and Pereira SA (2017) Implications of sulfotransferase activity in interindividual variability in drug response: clinical perspective on current knowledge. *Drug Metab Rev* **49:**357-371.

McCarver DG and Hines RN (2002) The ontogeny of human drug-metabolizing enzymes: phase II conjugation enzymes and regulatory mechanisms. *J Pharmacol Exp Ther* **300:**361-366.

Meloche CA, Sharma V, Swedmark S, Andersson P, and Falany CN (2002) Sulfation of budesonide by human cytosolic sulfotransferase, dehydroepiandrosterone-sulfotransferase (DHEA-ST). *Drug Metab Dispos* **30:**582-585.

Miller R, Roberts R, and Fischer L (1976) Acetaminophen elimination kinetics in neonates, children, and adults. *Clin Pharmacol Ther* **19:**284-294.

Mutlib AE, Goosen TC, Bauman JN, Williams JA, Kulkarni S, and Kostrubsky S (2006) Kinetics of acetaminophen glucuronidation by UDP-glucuronosyltransferases 1A1, 1A6, 1A9 and 2B15. Potential implications in acetaminophen-induced hepatotoxicity. *Chem Res Toxicol* **19:**701-709.

Nakamura Y, Gang HX, Suzuki T, Sasano H, and Rainey WE (2009) Adrenal changes associated with adrenarche. *Rev Endocr Metab Disord* **10:**19.

Nishimuta H, Ohtani H, Tsujimoto M, Ogura K, Hiratsuka A, and Sawada Y (2007) Inhibitory effects of various beverages on human recombinant sulfotransferase isoforms SULT1A1 and SULT1A3. *Biopharm Drug Dispos* **28:**491-500.

Nishiyama T, Ogura K, Nakano H, Ohnuma T, Kaku T, Hiratsuka A, Muro K, and Watabe T (2002) Reverse geometrical selectivity in glucuronidation and sulfation of cis-and trans-4-hydroxytamoxifens by human liver UDP-glucuronosyltransferases and sulfotransferases. *Biochem Pharmacol* **63:**1817-1830.

Nowell S and Falany C (2006) Pharmacogenetics of human cytosolic sulfotransferases. *Oncogene* **25:**1673.

Pacifici G, Franchi M, Giuliani L, and Rane A (1989) Development of the glucuronyltransferase and sulphotransferase towards 2-naphthol in human fetus. *Dev Pharmacol Ther* **14:**108-114.

Pacifici G, Kubrich M, Giuliani L, De Vries M, and Rane A (1993) Sulphation and glucuronidation of ritodrine in human foetal and adult tissues. *Eur J Clin Pharmacol* **44:**259-264.

Pacifici G, Säwe J, Kager L, and Rane A (1982) Morphine glucuronidation in human fetal and adult liver. *Eur J Clin Pharmacol* **22:**553-558.

Pacifici GM (2005) Sulfation of drugs and hormones in mid-gestation human fetus. *Early Hum Dev* **81:**573-581.

Pearce RE, Gaedigk R, Twist GP, Dai H, Riffel AK, Leeder JS, and Gaedigk A (2016) Developmental expression of CYP2B6: a comprehensive analysis of mRNA expression, protein content and bupropion hydroxylase activity and the impact of genetic variation. *Drug Metab Dispos* **44:**948-958.

Perucca E and Richens A (1979) Paracetamol disposition in normal subjects and in patients treated with antiepileptic drugs. *Br J Clin Pharmacol* **7:**201-206.

Prasad B, Gaedigk A, Vrana M, Gaedigk R, Leeder JS, Salphati L, Chu X, Xiao G, Hop CE, and Evers R (2016) Ontogeny of hepatic drug transporters as quantified by LC‐MS/MS proteomics. *Clin Pharmacol Ther* **100:**362-370.

Prasad B and Unadkat J (2015) The concept of fraction of drug transported (ft) with special emphasis on BBB efflux of CNS and antiretroviral drugs. *Clin Pharmacol Ther* **97:**320-323.

Prescott L (1980) Kinetics and metabolism of paracetamol and phenacetin. *Br J Clin Pharmacol* **10:**291S-298S.

Prescott L (1983) Paracetamol overdosage. *Drugs* **25:**290-314.

Prescott L, Speirs G, Critchley J, Temple R, and Winney R (1989) Paracetamol disposition and metabolite kinetics in patients with chronic renal failure. *Eur J Clin Pharmacol* **36:**291-297.

Rainey WE, Carr BR, Sasano H, Suzuki T, and Mason JI (2002) Dissecting human adrenal androgen production. *Trends Endocrinol Metab* **13:**234-239.

Rawlins M, Henderson D, and Hijab A (1977) Pharmacokinetics of paracetamol (acetaminophen) after intravenous and oral administration. *Eur J Clin Pharmacol* **11:**283-286.

Remer T, Boye KR, Hartmann MF, and Wudy SA (2005) Urinary markers of adrenarche: reference values in healthy subjects, aged 3-18 years. *J Clin Endocrinol Metab* **90:**2015-2021.

Richard K, Hume R, Kaptein E, Stanley EL, Visser TJ, and Coughtrie MW (2001) Sulfation of thyroid hormone and dopamine during human development:

ontogeny of phenol sulfotransferases and arylsulfatase in liver, lung, and brain. *J Clin Endocrinol Metab* **86:**2734-2742.

Rømsing J, Østergaard D, Senderovitz T, Drozdziewicz D, Sonne J, and Ravn G (2001) Pharmacokinetics of oral diclofenac and acetaminophen in children after surgery. *Paediatr Anaesth* **11:**205-213.

Rostami-Hodjegan A, Shiran M, Ayesh R, Grattan T, Burnett I, Darby-Dowman A, and Tucker G (2002) A new rapidly absorbed paracetamol tablet containing sodium bicarbonate. I. A four-way crossover study to compare the concentration-time profile of paracetamol from the new paracetamol/sodium bicarbonate tablet and a conventional paracetamol tablet in fed and fasted volunteers. *Drug Dev Ind Pharm* **28:**523-531.

Salem F, Johnson TN, Barter ZE, Leeder JS, and Rostami‐Hodjegan A (2013) Age related changes in fractional elimination pathways for drugs: assessing the impact of variable ontogeny on metabolic drug-drug interactions. *J Clin Pharmacol* **53:**857-865.

Saner KJ, Suzuki T, Sasano H, Pizzey J, Ho C, Strauss III JF, Carr BR, and Rainey WE (2005) Steroid sulfotransferase 2A1 gene transcription is regulated by steroidogenic factor 1 and GATA-6 in the human adrenal. *Mol Endocrinol* **19:**184-197.

Schrag ML, Cui D, Rushmore TH, Shou M, Ma B, and Rodrigues AD (2004) Sulfotransferase 1E1 is a low K_m isoform mediating the 3-O-sulfation of ethinyl estradiol. *Drug Metab Dispos* **32:**1299-1303.

Senggunprai L, Yoshinari K, and Yamazoe Y (2009) Selective role of SULT2A1 in the N-sulfoconjugation of quinolone drugs in human. *Drug Metab Dispos* **37:**1711-1717.

Shirasaka Y, Chaudhry AS, McDonald M, Prasad B, Wong T, Calamia JC, Fohner A, Thornton TA, Isoherranen N, and Unadkat JD (2016) Interindividual variability of CYP2C19-catalyzed drug metabolism due to differences in gene diplotypes and cytochrome P450 oxidoreductase content. *Pharmacogenomics J* **16:**375.

Singla NK, Parulan C, Samson R, Hutchinson J, Bushnell R, Beja EG, Ang R, and Royal MA (2012) Plasma and cerebrospinal fluid pharmacokinetic parameters after single‐dose administration of intravenous, oral, or rectal acetaminophen. *Pain Pract* **12:**523-532.

Stanley EL, Hume R, and Coughtrie MW (2005) Expression profiling of human fetal cytosolic sulfotransferases involved in steroid and thyroid hormone metabolism and in detoxification. *Mol Cell Endocrinol* **240:**32-42.

Umehara K-i, Huth F, Gu H, Schiller H, Heimbach T, and He H (2017) Estimation of fractions metabolized by hepatic CYP enzymes using a concept of inter-system extrapolation factors (ISEFs)-a comparison with the chemical inhibition method. *Drug Metab Pers Ther* **32:**191-200.

Upreti VV and Wahlstrom JL (2016) Meta‐analysis of hepatic cytochrome P450 ontogeny to underwrite the prediction of pediatric pharmacokinetics using physiologically based pharmacokinetic modeling. *J Clin Pharmacol* **56:**266-283.

Villiger A, Stillhart C, Parrott N, and Kuentz M (2016) Using physiologically based pharmacokinetic (PBPK) modelling to gain insights into the effect of physiological factors on oral absorption in paediatric populations. *AAPS J* **18:**933-947.

Vrana M, Whittington D, Nautiyal V, and Prasad B (2017) Database of optimized proteomic quantitative methods for human drug disposition‐related proteins

for applications in physiologically based pharmacokinetic modeling. *CPT Pharmacometrics Syst Pharmacol* **6:**267-276.

Wang J, Falany JL, and Falany CN (1998) Expression and characterization of a novel thyroid hormone-sulfating form of cytosolic sulfotransferase from human liver. *Mol Pharmacol* **53:**274-282.

Wong T, Wang Z, Chapron BD, Suzuki M, Claw KG, Gao C, Foti RS, Prasad B, Chapron A, and Calamia J (2018) Polymorphic human sulfotransferase 2A1 mediates the formation of 25-hydroxyvitamin D3-3-O-sulfate, a major circulating vitamin D metabolite in humans. *Drug Metab Dispos* **46(**367-379.

Yang J, Jamei M, Yeo KR, Rostami-Hodjegan A, and Tucker GT (2007) Misuse of the well-stirred model of hepatic drug clearance. *Drug Metab Dispos* **35:**501-502.

Zapater P, Lasso De La Vega M, Horga J, Such J, Frances R, Esteban A, Palazon J, Carnicer F, Pascual S, and Pérez‐Mateo M (2004) Pharmacokinetic variations of acetaminophen according to liver dysfunction and portal hypertension status. *Aliment Pharmacol Ther* **20:**29-36.

Zuppa AF, Hammer GB, Barrett JS, Kenney BF, Kassir N, Mouksassi S, and Royal MA (2011) Safety and population pharmacokinetic analysis of intravenous acetaminophen in neonates, infants, children, and adolescents with pain or fever. *J Pediatr Pharmacol Ther* **16:**246-261.

Zurlinden TJ and Reisfeld B (2016) Physiologically based modeling of the pharmacokinetics of acetaminophen and its major metabolites in humans using a Bayesian population approach. *Eur J Drug Metab Pharmacokinet* **41:**267-280.

Footnotes

The proteomics and genotyping work was funded by a grant from Eunice Kennedy Shriver National Institute of Child Health and Human Development [R01.HD081299]. The National Institute of Child Health and Human Development Brain and Tissue Bank for Developmental Disorders at the University of Maryland was funded by the National Institutes of Health (NIH) contract [N01-HD-9-0011/HHSN275200900011C], and the Liver Tissue Cell Distribution System are funded by NIH contract [N01-DK-7- 0004/HHSN267200700004C]. Financial assistance for the Ph.D. fellowship to M.K.L. for PBPK modeling work was provided by Bristol-Myers Squibb [NIPER SP-215].

Figure legends

Figure 1. Age-dependent abundance (categorical) of SULT1A1 (A), SULT1A3 (B), SULT1B1 (C) and SULT2A1 (D) across 6 developmental periods, i.e., neonatal (0 to 27 days); infancy (28 to 364 days); toddler/early childhood (1 to <6 years); middle childhood (6 to <12 years); adolescence (12 to 18 years), and adulthood (>18 years). Statistical analysis for inter-comparison of enzyme abundance across different age groups was performed using Kruskal-Wallis test followed by Dunn's multiple comparison test. The number of samples in each age category is indicated in parentheses on the x-axis. Data for SULT1A1 and SULT2A1 represent absolute protein levels (determined using protein standard calibrator), whereas SULT1A3 and SULT1B1 data are presented as relative data (normalized by pooled quality control values). *, ** and *** represent p-value <0.05, <0.01 and <0.001, respectively.

Figure 2. Association of ethnicity with human hepatic SULT1A1 (A), SULT1A3 (B), SULT1B1 (C), and SULT2A1 (D) protein levels. Statistical analysis for inter-comparison of abundance among the two ethnic groups was performed through Mann Whitney test. The number of samples in each ethnicity category is indicated in parentheses on the x-axis. *** represents p-value <0.001.

Figure 3. Observed *versus* predicted dose-normalized acetaminophen plasma concentration-time profiles of IV infusion (2 hours) (A); oral solution-fasted state (B); oral tablet-fasted state (C), and oral tablet-fed state (D) dosing in adults. These profiles were generated by dividing the observed or predicted plasma concentrations by the dose. The gastric emptying time considered for the fed-state was 1 hour, whereas for the oral tablet and oral solution, it was considered to be 15 min and 6 min, respectively. The symbols represent observed data, while the solid lines indicate the model predicted mean profile. The dotted and dashed lines represent the predicted profiles when lower and upper 95% CI of protein abundances of UGTs, SULTs and CYPs (age >18 years) were considered for metabolism-related interindividual variability in adults. Abbreviations used in the legends represent the following: L1 (5 mg/kg, predicted-fasted state); L2 (5 mg/kg (Clements et al.,

1984)); L3 (20 mg/kg (Clements et al., 1984)); L4 (1000 mg, predicted-fasted state); L5 (1000 mg (Kamali et al., 1992)); L6 (1000 mg (Prescott et al., 1989)); L7 (12 mg/kg (Prescott, 1980)); L8 (5 mg/kg, predicted-fasted state); L9 (500 mg (Rawlins et al., 1977)); L10 (1000 mg (Rawlins et al., 1977)); L11 (2000 mg (Rawlins et al., 1977)); L12 (1000 mg (Singla et al., 2012)); L13 (1000 mg (Zapater et al., 2004)); L14 (1000 mg (Rostami-Hodjegan et al., 2002)); L15 (1000 mg, predicted-fed state), and L16 (1000 mg (Rostami-Hodjegan et al., 2002)).

Figure 4. Observed *versus* predicted plasma concentration-time profiles of acetaminophen in neonates and infants for the mentioned doses. The drug was delivered as IV infusion for 15 min in case of all the figures, except (C) where the duration of infusion was 50 min. Also, separately indicated as bar diagrams is the comparison of mean predicted (without and with proteomics based ontogeny data) and observed (L20) C_{max} (G), and AUC_{0-6} (H) values for 15 mg/kg acetaminophen administered as IV infusion for 15 minutes to neonates and infants. In this case, the average age values for neonates and infants were considered as 14 days and 1 year, respectively, in accordance with US-FDA label (CDER, 2010). Abbreviations used in the legends represent the following literature references: L17 (Zuppa et al., 2011); L18 (Cook et al., 2016); L19 (Allegaert et al., 2013), and L20 (CDER, 2010).

Figure 5. Ontogeny-based predicted f_m values of acetaminophen metabolizing enzymes across different age-groups (neonatal to adulthood) after oral administration of 10 mg/kg drug solution, as estimated in this study (shown by pie charts A-F). The pie charts are shown in different diameters so as to represent magnitude of apparent clearance ($CL/F= Dose/AUC_{0-inf}$). The predicted f_m values were further confirmed by comparison of observed and predicted urinary recoveries (A_e, mmol) of acetaminophen (APAP), acetaminophen-sulfate (APAP-S) and acetaminophen-glucuronide (APAP-G) across different age-groups (shown as bar diagrams G-L). The predicted A_e data were generated in respective age groups after consideration of mean (bar), and 95% CI (error bars) protein abundance data. Dots indicate observed urinary elimination data. Abbreviations used in the legends represent the following:

L21 (Miller et al., 1976); L22 (Alam et al., 1977); L23 (Clements et al., 1984); L24 (Critchley et al., 1986), and L25 (Critchley et al., 2005).

Tables

Table 1. Hepatic SULT protein abundance data with demographic details*.

	Median	Min	Max	Mean	SD	%CV	SE	SF	Lower 95% CI	Higher 95% CI
SULT1A1										
All samples (190)	387.0	27.1	1658.0	445.2	281.1	63.1	20.4	NA	404.9	485.4
Neonatal (4)	99.1	57.6	126.8	95.7	28.8	30.1	14.4	0.24	49.8	141.5
Infancy (17)	189.2	52.2	824.0	323.1	254.1	78.6	61.6	0.80	192.4	453.7
Toddler/early childhood (29)	610.3	113.5	1658.0	639.2	333.4	52.2	61.9	1.57	512.4	766.1
Middle childhood (37)	512.0	30.8	1046.0	506.4	283.5	56.0	46.6	1.25	411.9	601.0
Adolescence (46)	338.7	27.1	1153.0	397.7	306.3	77.0	45.2	0.98	306.7	488.7
Adulthood (57)	370.9	147.6	1116.0	405.9	163.7	40.3	21.7	1.00	362.5	449.3
Female (73)	394.4	30.8	1240.0	450.6	258.7	57.4	30.3	NA	390.2	510.9
Male (115)	376.9	27.1	1658.0	442.8	297.6	67.2	27.8	NA	387.8	497.8
African American (29)	313.2	78.6	792.3	348.7	233.9	67.1	43.4	NA	259.7	437.6
Caucasian (120)	358.7	27.1	1116.0	386.3	231.4	59.9	21.1	NA	344.4	428.1
CNV 1 (5)	219.2	121.4	376.4	245.1	108.2	44.1	48.4	NA	110.7	379.5
CNV 2 (82)	387.0	27.1	1153.0	434.6	298.0	68.6	32.9	NA	369.2	500.1

CNV 3 (28)	577.3	72.6	1240.0	534.4	347.6	65.0	65.7	NA	399.6	669.1
CNV 4 (7)	506.4	146.8	1658.0	573.1	536.0	93.5	202.6	NA	77.3	1069.0
SULT1A3										
All samples (190)	95.7	16.9	484.7	98.1	60.7	61.9	4.4	NA	89.4	106.8
Neonatal (4)	40.9	30.0	81.5	48.3	23.1	47.7	11.5	0.47	11.6	85.0
Infancy (17)	40.9	27.2	256.8	77.8	75.2	96.6	18.2	0.76	39.2	116.5
Toddler/early childhood (29)	109.2	25.7	330.2	116.2	74.2	63.9	13.8	1.14	87.9	144.4
Middle childhood (37)	95.5	16.9	229.0	101.5	54.8	54.0	9.0	0.99	83.3	119.8
Adolescence (46)	77.2	22.6	484.7	90.5	80.8	89.2	11.9	0.88	66.5	114.5
Adulthood (57)	101.6	71.5	181.2	102.3	18.2	17.7	2.4	1.00	97.5	107.1
Female (75)	97.8	16.9	330.2	98.2	53.0	54.0	6.1	NA	86.0	110.4
Male (113)	92.9	22.6	484.7	98.3	66.0	67.1	6.2	NA	86.0	110.6
African American (28)	39.3	23.6	128.5	55.6	32.8	59.0	6.2	NA	42.9	68.4
Caucasian (119)	94.6	22.6	282.8	94.6	49.8	52.6	4.6	NA	85.5	103.6
SULT1B1										
All samples (191)	99.9	16.7	364.7	109.1	65.6	60.1	4.7	NA	99.7	118.4
Neonatal (3)	19.2	16.7	28.2	21.4	6.0	28.3	3.5	0.19	6.3	36.4

Infancy (17)	40.8	20.6	123.5	47.4	26.6	56.1	6.5	0.41	33.7	61.1
Toddler/early childhood (30)	110.1	26.4	338.0	128.5	75.0	58.4	13.7	1.12	100.5	156.5
Middle childhood (37)	117.8	19.4	269.1	114.9	57.2	49.8	9.4	1.00	95.8	134.0
Adolescence (47)	90.9	19.8	364.7	113.2	85.2	75.3	12.4	0.99	88.2	138.3
Adulthood (57)	114.7	43.9	222.2	114.6	39.5	34.4	5.2	1.00	104.1	125.1
Female (75)	99.5	19.2	338.0	109.7	56.5	51.5	6.5	NA	96.7	122.7
Male (114)	104.6	16.7	364.7	108.9	71.6	65.8	6.7	NA	95.6	122.2
African American (28)	55.3	16.7	134.2	60.0	32.4	54.0	6.1	NA	47.4	72.5
Caucasian (121)	98.7	19.2	231.3	102.2	53.6	52.5	4.9	NA	92.6	111.9
rs11249460_C/C (26)#	122.3	68.7	222.2	127.6	41.6	32.6	8.2	NA	110.8	144.3
rs11249460_C/T (29)#	108.4	43.9	186.1	103.3	33.8	32.7	6.3	NA	90.4	116.2
rs11249460_T/T (4)#	99.7	67.6	123.9	97.7	23.2	23.8	11.6	NA	60.7	134.7
SULT2A1										
All samples (183)	1065.0	80.0	4085.0	1290.0	829.0	64.3	61.3	NA	1169.0	1411.0
Neonatal (4)	453.3	158.4	617.0	420.5	193.8	46.1	96.9	0.38	112.1	728.8
Infancy (17)	1012.0	80.0	4085.0	1249.0	987.3	79.0	239.5	1.11	741.3	1757.0
Toddler/early childhood (29)	1885.0	160.4	3714.0	1832.0	1019.0	55.6	189.2	1.63	1444.0	2220.0

Middle childhood (37)	1209.0	230.1	3949.0	1460.0	997.0	68.3	163.4	1.30	1128.0	1793.0
Adolescence (42)	882.3	128.7	2885.0	1082.0	726.9	67.2	112.4	0.97	855.2	1308.0
Adulthood (54)	1060.0	260.9	2071.0	1121.0	359.5	32.1	48.9	1.00	1023.0	1219.0
Female (74)	1035.0	160.4	3949.0	1306.0	801.6	61.4	93.2	NA	1120.0	1492.0
Male (107)	1080.0	80.0	4085.0	1284.0	857.7	66.8	82.9	NA	1120.0	1449.0
African American (28)	853.5	80.0	3066.0	956.6	687.2	71.8	129.9	NA	690.1	1223.0
Caucasian (117)	1036.0	95.6	4085.0	1185.0	747.9	63.1	69.1	NA	1048.0	1322.0

*The number of samples in each category is indicated in parentheses. Median and mean values for SULT1A1/SULT2A1 are expressed in pmol/mg cytosol protein, while those for SULT1B1/ SULT1A3 are expressed in relative value (normalized by the pooled quality control values). Mean adult abundance value was taken as 1 to calculate SF for all the SULTs. Only SNPs with significant association with protein abundance are tabulated here (see also supplementary Figures 3S and 4S for SNPs and CNV, respectively). Abbreviations: Min (minimum), Max (maximum), SD (standard deviation), %CV (percent coefficient variation), SE (standard error), SF (scale factor) and 95% CI (95% confidence interval).

Table 2. Comparison of acetaminophen PBPK model predicted and observed PK data*.

Study ID	Dose	Parameters	Mean observed value (O)	Acceptance range	Mean predicted value (P)	P/O ratio	Compliance to model evaluation criteria		
							Bioequivalence criteria	2-fold criteria	Population criteria
IV (adults)									
1	5 mg/kg	AUC (0-inf, h)	18.38	15.50-21.80	18.42	1.00	Yes	Yes	Yes
1	20 mg/kg	AUC (0-inf, h)	82.48	77.85-87.38	74.83	0.91	Yes	Yes	Yes
2	1000 mg	C_{max}	21.6	15.86-29.42	30.01	1.39	No	Yes	No
2	1000 mg	AUC (0-inf, h)	42.5	31.96-56.52	42.22	0.99	Yes	Yes	Yes
3	1000 mg	AUC (0-inf, h)	50.5	31.50-80.96	53.42	1.06	Yes	Yes	Yes
4	1000 mg	C_{max}	55.3	47.78-64.00	44.99	0.81	No	Yes	No
5	12 mg/kg	AUC (0-inf, h)	36.7	34.23-39.35	44.76	1.22	No	Yes	No
Oral tablet (adults)									
2	1000 mg	C_{max}	12.3	6.14-24.63	11.15	0.91	Yes	Yes	Yes
2	1000 mg	AUC (0-6 h)	29.4	13.32-64.89	35.80	1.22	Yes	Yes	Yes
3	500 mg	AUC (0-inf, h)	15.6	6.53-37.27	22.93	1.47	No	Yes	Yes
3	1000 mg	AUC (0-inf, h)	44	30.87-62.72	46.40	1.05	Yes	Yes	Yes
3	2000 mg	AUC (0-inf, h)	87.6	48.32-158.81	94.54	1.08	Yes	Yes	Yes
6	1000 mg	C_{max}	15.9	11.20-22.57	11.15	0.70	No	Yes	No
6	1000 mg	AUC (0-6 h)	38.8	32.48-46.35	35.80	0.92	Yes	Yes	Yes
7	1000 mg	C_{max}	18	11.86-27.33	11.15	0.62	No	Yes	No
7	1000 mg	AUC (0-inf, h)	54.78	45.35-66.17	46.40	0.85	Yes	Yes	Yes
8	500 mg	C_{max}	5.65	3.38-9.46	5.54	0.98	Yes	Yes	Yes
8	500 mg	C_{max}	4.7	3.64-6.06	5.54	1.18	Yes	Yes	Yes
Oral tablet (adults)-fed state									
7	1000 mg	C_{max}	11	8.87-13.65	7.47	0.68	No	Yes	No
7	1000 mg	AUC (0-inf, h)	51.92	43.51-61.95	46.44	0.89	Yes	Yes	Yes
Oral solution (adults)									

9	1000 mg	C_{max}	17.5	9.22-33.23	13.70	0.78	Yes	Yes	Yes
10	1000 mg	C_{max}	20	11.62-34.42	13.70	0.69	No	Yes	Yes
10	1000 mg	AUC (0-24 h)	45	32.53-62.25	46.37	1.03	Yes	Yes	Yes
4	1000 mg	AUC (0-inf, h)	49.4	42.31-57.68	46.51	0.94	Yes	Yes	Yes
5	12 mg/kg	AUC (0-inf, h)	28	18.09-43.33	38.93	1.39	No	Yes	Yes
IV (neonates)									
11	15 mg/kg	C_{max}	25	8.88-70.35	24.75	0.99	Yes	Yes	Yes
11	15 mg/kg	AUC (0-6 h)	62	52.91-72.65	68.66	1.11	Yes	Yes	Yes
IV (infants)									
11	15 mg/kg	C_{max}	29	10.64-79.07	27.78	0.96	Yes	Yes	Yes
11	15 mg/kg	AUC (0-6 h)	57	40.93-79.38	53.51	0.94	Yes	Yes	Yes
IV (children)									
11	15 mg/kg	C_{max}	29	23.32-36.07	28.31	0.98	Yes	Yes	Yes
11	15 mg/kg	AUC (0-6 h)	38	32.80-44.02	47.33	1.25	Yes	Yes	No
IV (adolescents)									
11	15 mg/kg	C_{max}	31	25.43-37.79	28.60	0.92	Yes	Yes	Yes
11	15 mg/kg	AUC (0-6 h)	41	33.81-49.71	52.83	1.29	No	Yes	No
PO tablet (middle childhood)									
12	22.5 mg/kg	C_{max}	12.7	8.56-18.84	19.75	1.55	No	Yes	No
12	22.5 mg/kg	AUC (0-4 h)	33.13	22.14-49.58	52.02	1.57	No	Yes	No

*Clinical studies were used as the training and qualification sets. The observed and the predicted C_{max} (µg/mL) and AUC (µg·h/mL) (mean, lower and upper 95% CI of the proteomics data of DMEs) for these studies are shown for all pediatric and adult populations and for the intravenous (IV) and oral (PO) routes of administration. The simulated mean C_{max} (µg/mL) and AUC (µg·h/mL) values were compared to the observed data and the acceptance criteria (based on bioequivalence criterion (1.25 fold), 2-fold criterion, and population-based criterion) was determined. Study ID in the table represent the following: 1 (Clements et al., 1984); 2 (Singla et al., 2012); 3 (Rawlins et al., 1977); 4 (Perucca and Richens, 1979); 5 (Prescott, 1980); 6 (Zapater et al., 2004); 7 (Rostami-Hodjegan et al., 2002); 8 (Manyike et al., 2000); 9 (Kamali et al., 1992); 10 (Prescott, 1980); 11 (CDER, 2010), and 12 (Rømsing et al., 2001).

DMD Fast Forward. Published on May 17, 2019 as DOI: 10.1124/dmd.119.086462
This article has not been copyedited and formatted. The final version may differ from this version.

Table 3. Ontogeny-based predicted UGT/SULT f_m values of acetaminophen across different age groups*.

Age groups (mean, range)	UGT/SULT f_m		
	Mean	**Lower 95%CI**	**Upper 95%CI**
Neonatal (14 days, 0 to 27 days)	0.46	0.12	0.55
Infancy (6 months, 28 to 364 days)	0.54	0.62	0.50
Infancy (1 year, 29 to <2 years)	0.44	0.49	0.42
Toddler/early childhood (4 years, 1 to <6 years)	0.47	0.45	0.48
Middle childhood (9 years, 6 to <12 years)	0.64	0.62	0.64
Children (7 years, 2 to <12 years)	0.56	0.56	0.56
Adolescence (14 years, 12 to 16 years)	1.02	1.18	0.91
Adolescence (15 years, 12 to 18 years)	0.97	1.08	0.90
Adulthood (30 years, >18 years)	1.71	1.60	1.86

*Mean, lower and upper 95% CI of the proteomics data of DMEs were considered for prediction of f_m of DMEs. Abbreviation: 95% CI (95% confidence interval).

DMD Fast Forward. Published on May 17, 2019 as DOI: 10.1124/dmd.119.086462
This article has not been copyedited and formatted. The final version may differ from this version.

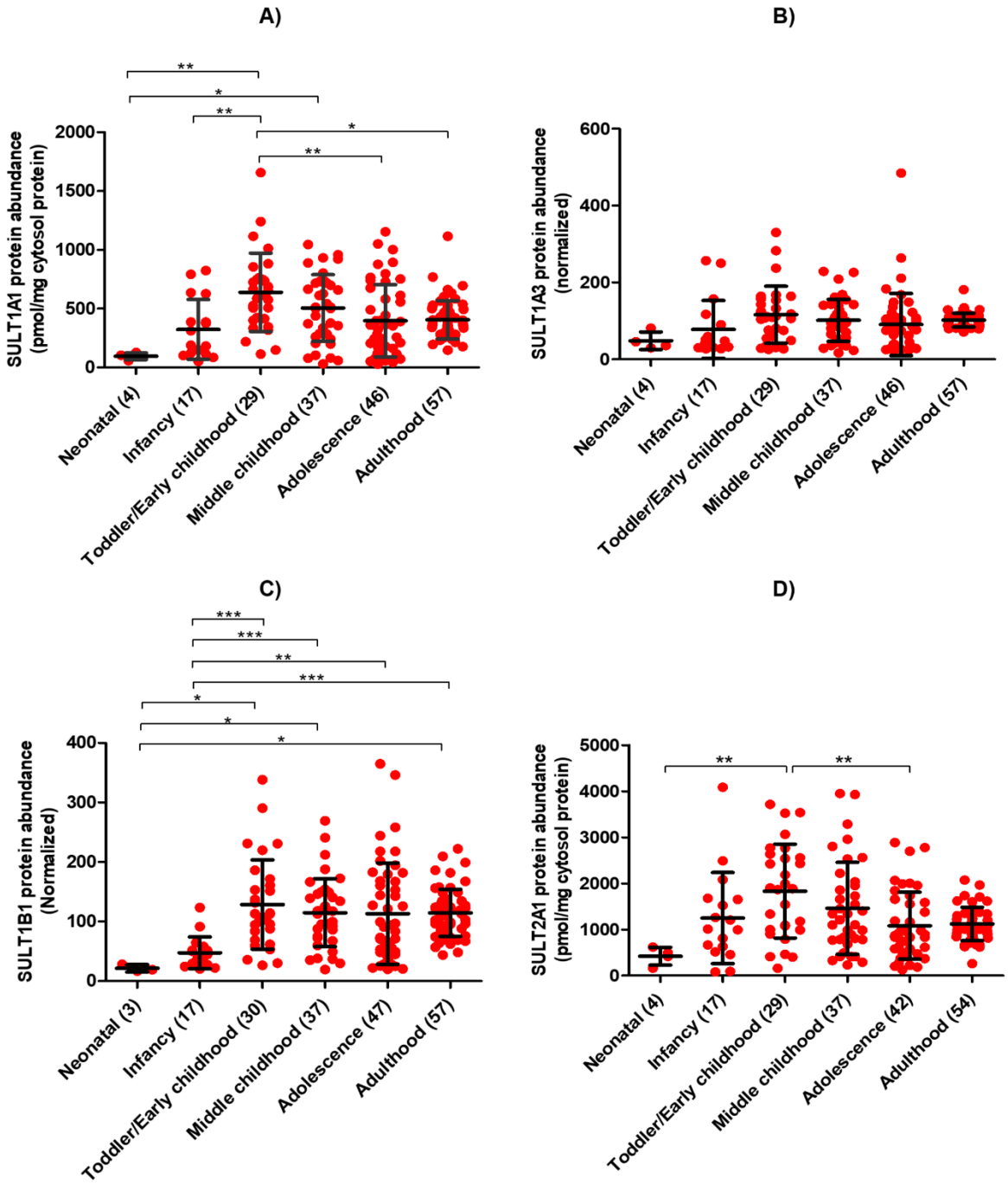

Figure 1.

DMD Fast Forward. Published on May 17, 2019 as DOI: 10.1124/dmd.119.086462
This article has not been copyedited and formatted. The final version may differ from this version.

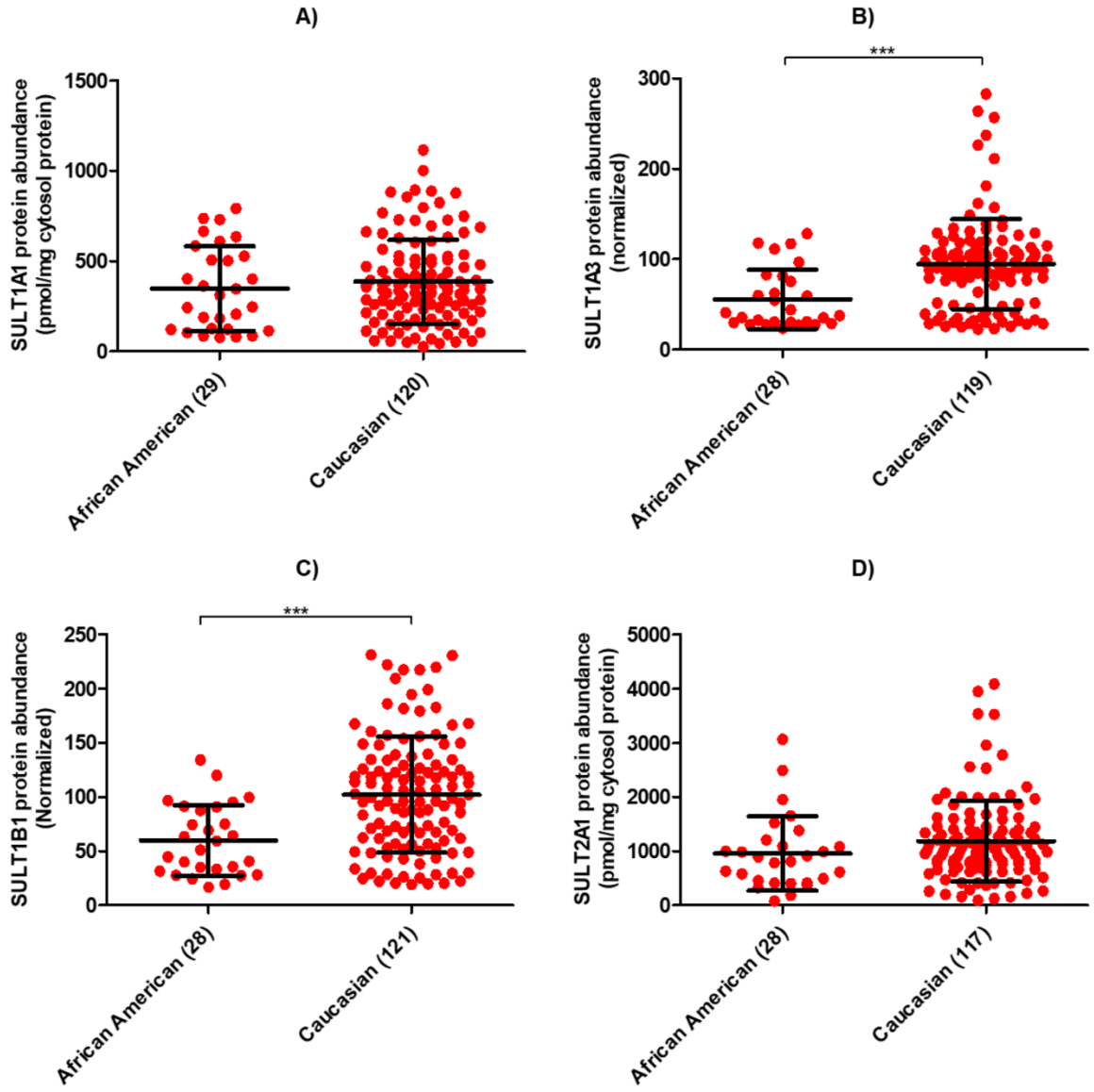

Figure 2.

DMD Fast Forward. Published on May 17, 2019 as DOI: 10.1124/dmd.119.086462
This article has not been copyedited and formatted. The final version may differ from this version.

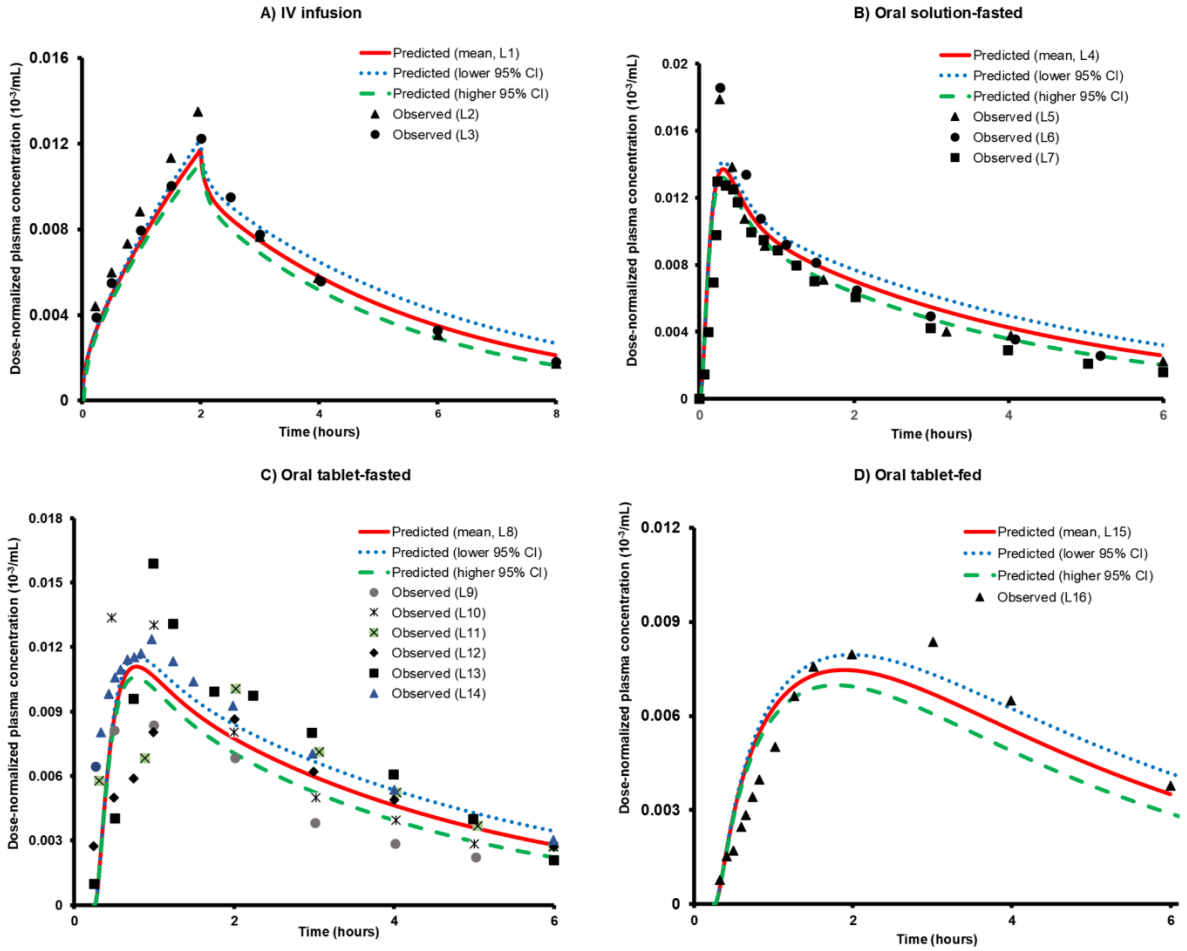

Figure 3.

DMD Fast Forward. Published on May 17, 2019 as DOI: 10.1124/dmd.119.086462
This article has not been copyedited and formatted. The final version may differ from this version.

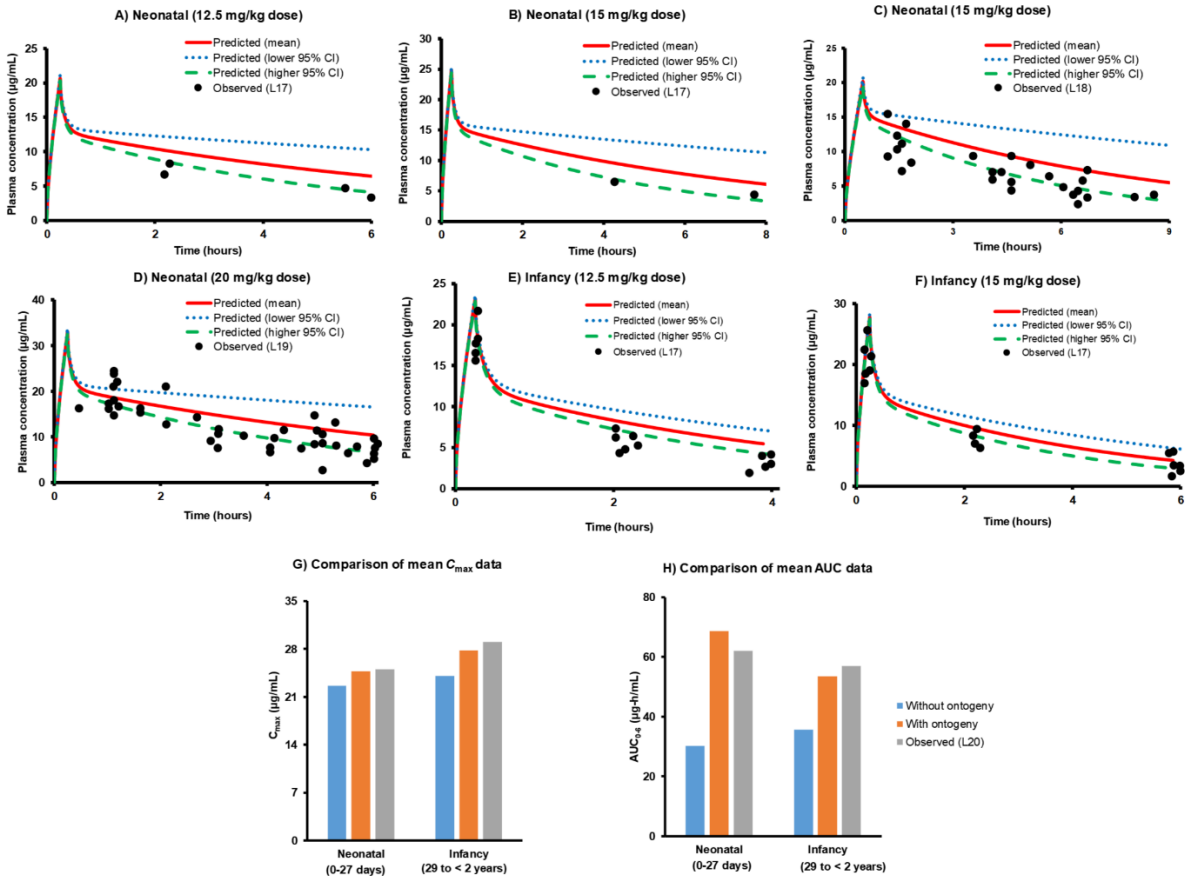

Figure 4.

DMD Fast Forward. Published on May 17, 2019 as DOI: 10.1124/dmd.119.086462
This article has not been copyedited and formatted. The final version may differ from this version.

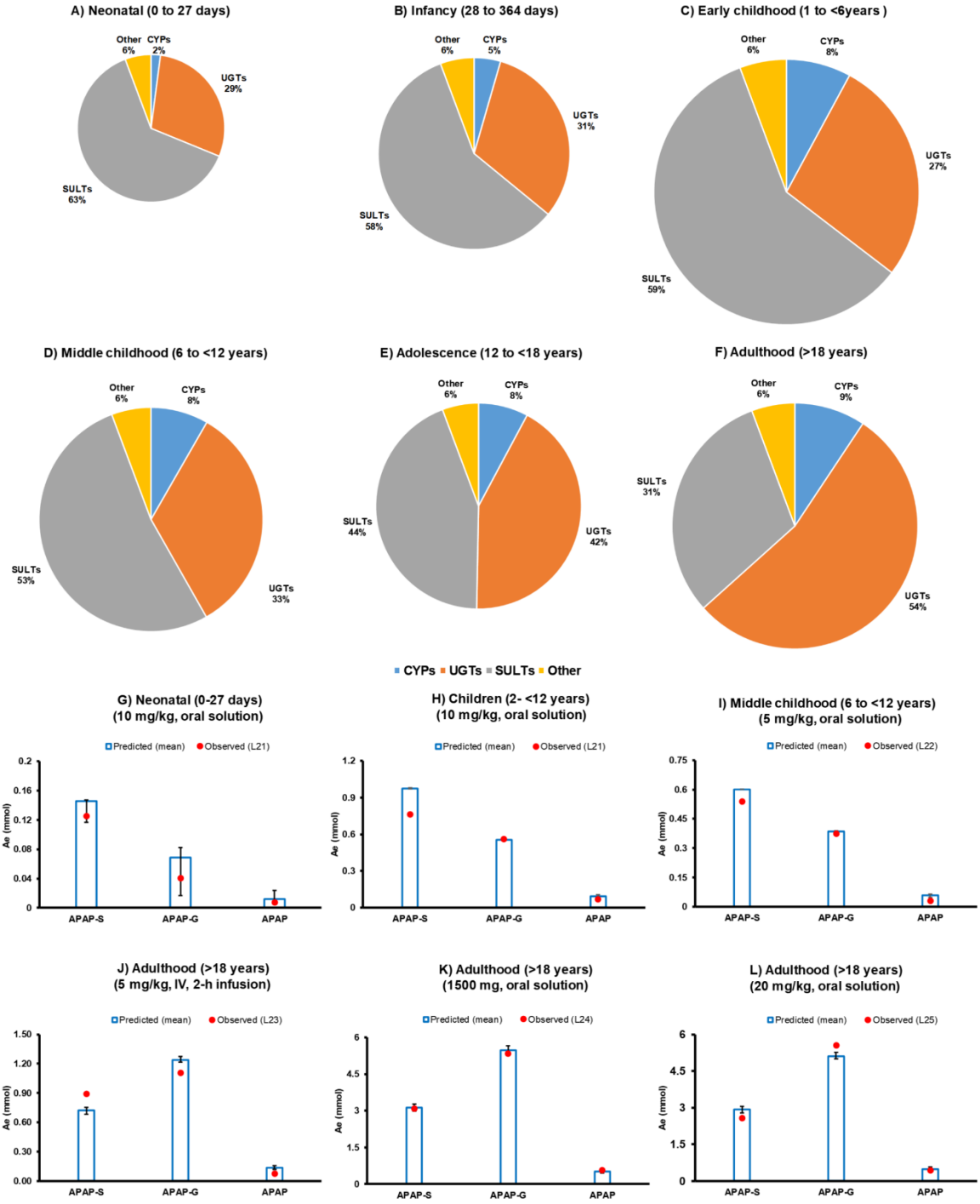

Figure 5.

SUPPLEMENTAL FILE

Ontogeny of Hepatic Sulfotransferases (SULTs) and Prediction of Age-Dependent Fractional Contribution of Sulfation in Acetaminophen Metabolism

Mayur K. Ladumor, Deepak Kumar Bhatt, Andrea Gaedigk, Sheena Sharma, Aarzoo Thakur, Robin E. Pearce, J. Steven Leeder, Michael B. Bolger, Saranjit Singh, and Bhagwat Prasad

Department of Pharmaceutical Analysis, National Institute of Pharmaceutical Education and Research (NIPER), Mohali, Punjab 160062, India (M.K.L., S.Sh, A.T. and S.Si)

Department of Pharmaceutics, University of Washington, Seattle, Washington 98195, USA (D.K.B. and B.P.)

Division of Clinical Pharmacology, Toxicology & Therapeutic Innovation, Department of Pediatrics, Children's Mercy Kansas City; and School of Medicine, University of Missouri-Kansas City, Kansas City, Missouri 64110, USA (A.G., R.E.P. and J.S.L.)

Simulations Plus, Inc., Lancaster, California 93534, USA (M.B.B.)

Running title: Age-dependent abundance of SULTs and its implications

Corresponding authors:

Bhagwat Prasad, Ph.D., Department of Pharmaceutics, University of Washington, Seattle, WA 98195, USA. Phone: +1-206-221-2295, E-mail: bhagwat@uw.edu

Saranjit Singh, Ph.D., Department of Pharmaceutical Analysis, National Institute of Pharmaceutical Education and Research (NIPER), Mohali (S.A.S. Nagar) 160062, Punjab, India. Phone: +91-172-2292031, E-mail: ssingh@niper.ac.in

Supplemental Methodology

Methodology for protein denaturation, reduction, alkylation, enrichment and trypsin digestion

The human liver cytosol (HLC) samples and purified SULT1A1 and SULT2A1 were digested using trypsin, as described in our previous publication (Bhatt et al., 2017). Briefly, 80 µL of HLC samples (2 mg/L) and serially diluted purified protein standards (SULT1A1 and SULT2A1) were incubated with 10 µL dithiothreitol (250 mM), 40 µL ammonium bicarbonate buffer (100 mM, pH 7.8) and 10 µL bovine serum albumin (2 mg/mL) at 95 °C for 10 min. 20 µL iodoacetamide (500 mM) was added to the incubate after cooling to the room temperature and so prepared solution was further incubated in the dark for 30 min at the same temperature. Sequentially, ice-cold methanol (500 µL), ice-cold chloroform (100 µL) and ice-cold deionized water (400 µL) were added. The samples were mixed, centrifuged at 16,000 g (4°C) for 5 min, and the upper and lower layers were discarded. The pellets were dried at room temperature for 10 min, followed by washing with ice-cold methanol (500 µL) and subsequent centrifugation at 8000 g (4°C) for 5 min. The supernatant layer was removed and the pellets were left to dry at room temperature for 30 minutes. These were then resuspended in a mixture of 60 µL ammonium bicarbonate buffer (50 mM, pH 7.8) and 20 µL trypsin (0.16 µg/µL). The samples were incubated at 37°C for 16 h (300 rpm). The reaction was quenched by placing samples in dry ice and adding heavy peptide internal standards, viz., 20 µL prepared in acetonitrile:water, 80:20 (v/v) containing 0.5% formic acid, and separately 10 µL prepared in acetonitrile:water (80:20 (v/v) containing 0.1% formic acid). The samples were mixed, centrifuged at 4000 g for 5 min (4°C), and transferred to LC-MS vials.

Fractional contribution of individual metabolic pathways and fractional contribution of UGT, SULT and CYP isoforms in acetaminophen metabolism in adults

Fractional contribution of individual metabolic pathways of acetaminophen metabolism in adults (i.e., $f_{m,UGT}$, $f_{m,SULT}$ and $f_{m,CYP}$) were derived from urinary recovery data (De Morais et al., 1992; Chen et al., 1998; Court et al., 2001; Mutlib et al., 2006; Adjei et al., 2008; Laine et al., 2009; Miners et al., 2011; Navarro et al., 2011; Jiang et al.,

2013). Isoform specific percent (%) contribution of UGT and CYP in acetaminophen metabolism in adults was derived from the literature data (De Morais et al., 1992; Chen et al., 1998; Court et al., 2001; Mutlib et al., 2006; Adjei et al., 2008; Laine et al., 2009; Miners et al., 2011; Navarro et al., 2011; Jiang et al., 2013). In case of CYPs, eqs. 1 and 2 were used for calculating the percent contribution of individual CYP isoforms.

$$\mathrm{CL_{int,CYP_j}} = \mathrm{CL_{int,rhCYP_j}} \times \mathrm{CYP_j\ abundance} \times \mathrm{ISEF_{CYP_j}} \quad (1)$$

$$\%\ \mathrm{Contribution\ of\ CYP} = \frac{\mathrm{CL_{int,CYP_j}}}{\sum \mathrm{CL_{int,CYP_j}}} \times 100 \quad (2)$$

where $CL_{int,CYPj}$ is intrinsic unbound clearance (µL/min/mg protein) of a drug by individual isoform of CYPs in human microsomes; $CL_{int,rhCYPj}$ is intrinsic unbound clearance of a drug by individual recombinant human CYP isoform (µL/min/pmol $rhCYP_j$) obtained from literature (De Morais et al., 1992; Chen et al., 1998; Court et al., 2001; Mutlib et al., 2006; Adjei et al., 2008; Laine et al., 2009; Miners et al., 2011; Navarro et al., 2011; Jiang et al., 2013); CYP_j abundance is the default GastroPlus value of protein abundance of individual CYP enzyme in liver microsomes, and $ISEF_{CYPj}$ is the inter-system extrapolation factor integrated to correct for differences in activity per unit enzyme between rhCYP and human microsomes (assumed as 1, a default value in GastroPlus).

In case of SULTs, eqs. 3 and 4 were employed for the determination of % contribution of individual SULT isoforms.

$$\mathrm{CL_{int,SULT_j}} = \frac{\mathrm{V_{max}}}{\mathrm{K_m}} = \frac{\mathrm{k_{cat}} \times \mathrm{SULT_j\ abundance}}{\mathrm{K_m}} \propto \frac{\mathrm{SULT_j\ abundance_{adult}}}{\mathrm{K_m}} \quad (3)$$

$$\%\ \mathrm{Contribution\ of\ SULT} = \frac{\mathrm{CL_{int,SULT_j}}}{\sum \mathrm{CL_{int,SULT_j}}} \times 100 \quad (4)$$

where $\mathrm{CL_{int,SULT_j}}$ is intrinsic clearance of a drug by individual isoform of SULTs; SULT $abundance_{adult}$ is the corresponding default healthy adult abundance values (pmol/mg

protein) of individual isoforms in liver tissue model of GastroPlus; K_m values were obtained from literature (De Morais et al., 1992; Chen et al., 1998; Court et al., 2001; Mutlib et al., 2006; Adjei et al., 2008; Laine et al., 2009; Miners et al., 2011; Navarro et al., 2011; Jiang et al., 2013), and k_{cat} is catalytic activity of the enzymes, which was assumed constant across SULT isoforms. Although k_{cat} can be different from one isoform to another, we assumed that protein abundance and K_m are the main determinants of the differential activities of individual SULT enzymes.

Supplemental Figure

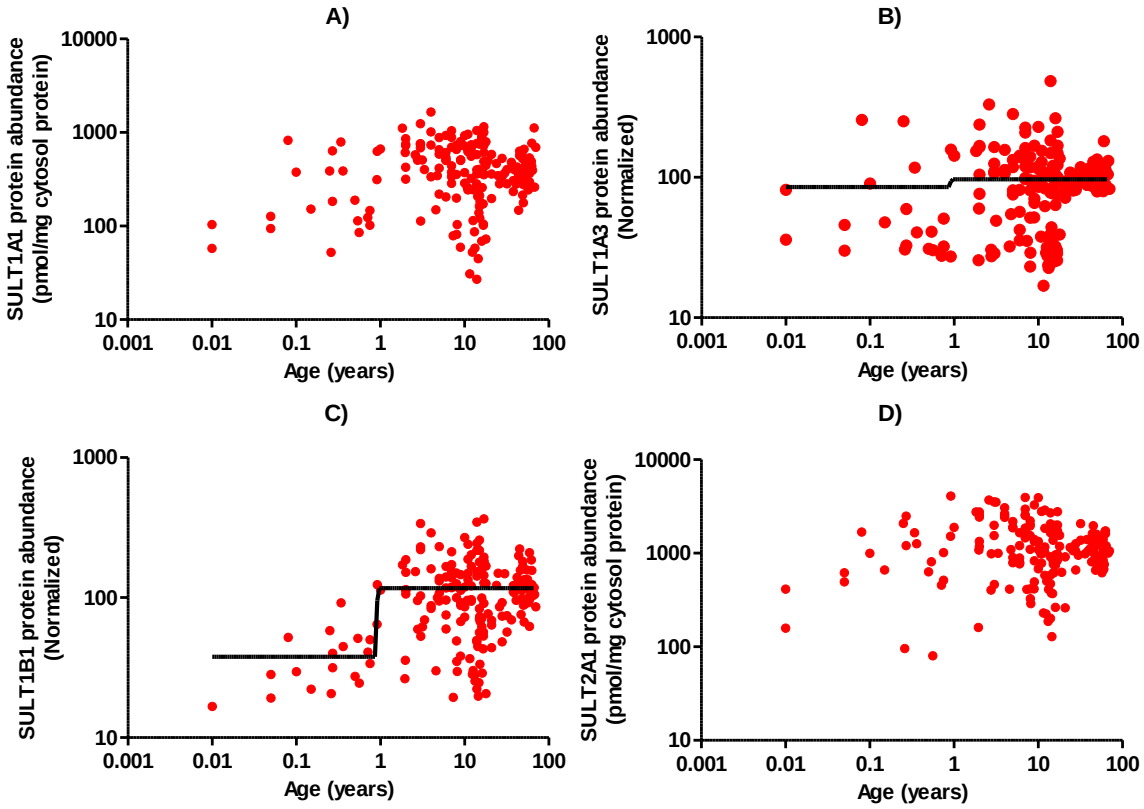

Supplemental Fig. 1. Age-dependent abundance (continuous scale) of SULT1A1 (A), SULT1A3 (B), SULT1B1 (C) and SULT2A1 (D). A non-linear allosteric sigmoidal model was fitted to the continuous age-dependent protein abundance data. Because of the high biological variability and high abundance in children, relative to infants and adults, allosteric model could not be optimized for SULT1A1 and SULT2A1.

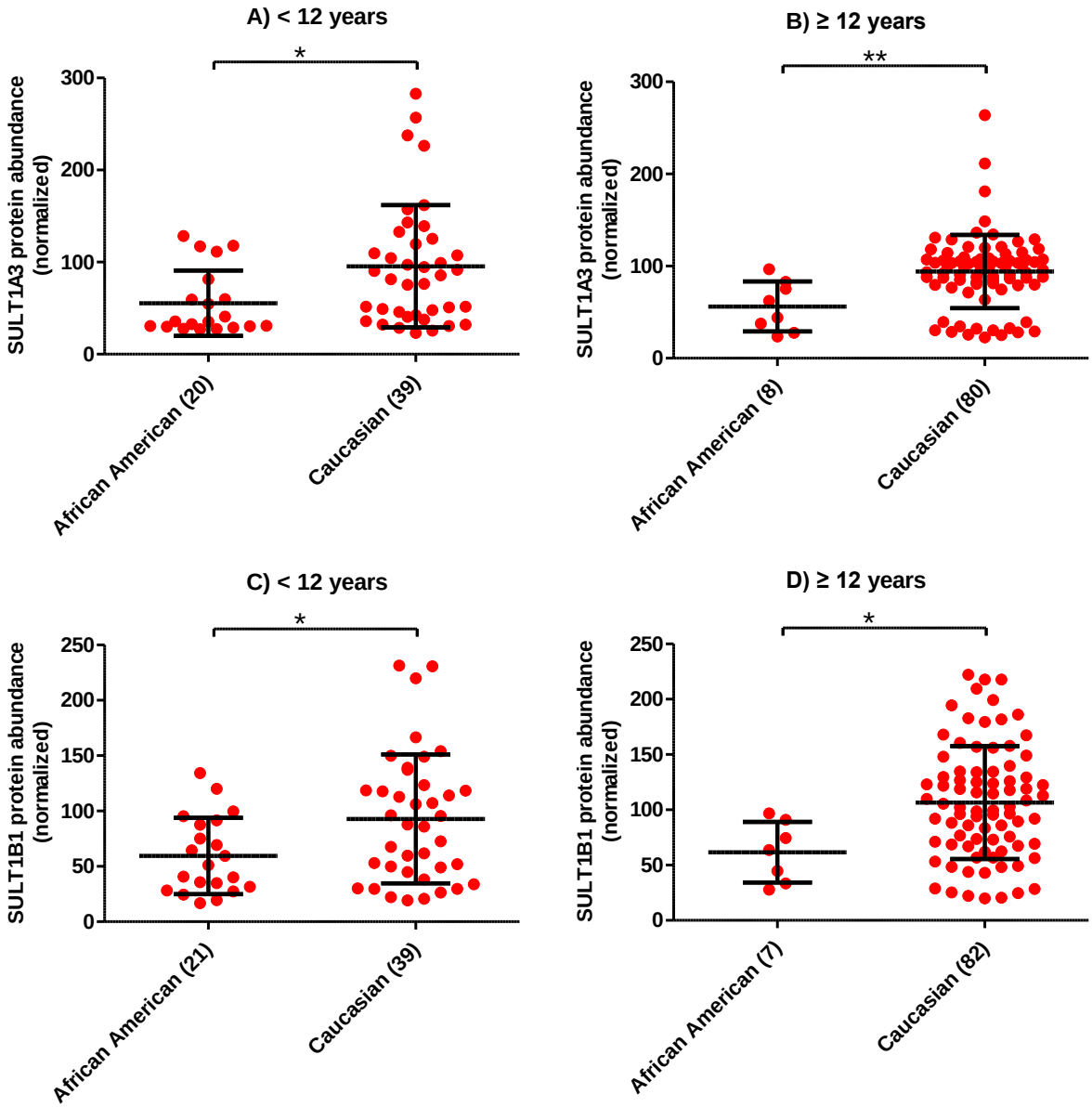

Supplemental Fig. 2. Association of ethnicity with human hepatic protein levels, viz., SULT1A3 of < 12 years (A), SULT1A3 of ≥ 12 years (B), SULT1B1 of < 12 years (C), and SULT1B1 of ≥ 12 years (D). Statistical analysis for inter-comparison of abundance among the two ethnic groups was performed through Mann-Whitney test. The number of samples in each ethnicity category is indicated in parentheses on the x-axis. * and ** represent p-value <0.05 and <0.01, respectively.

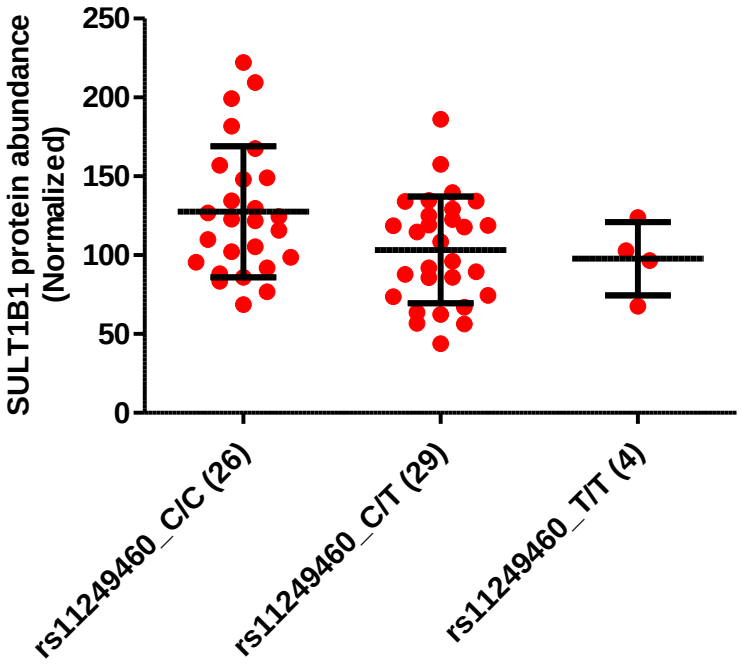

Supplemental Fig. 3. Association of genotype with hepatic SULT1B1 protein abundance in adults. Statistical analysis was performed using Kruskal-Wallis test followed by Dunn's multiple comparison test. The number of samples in each genotype category is indicated in parentheses on the x-axis.

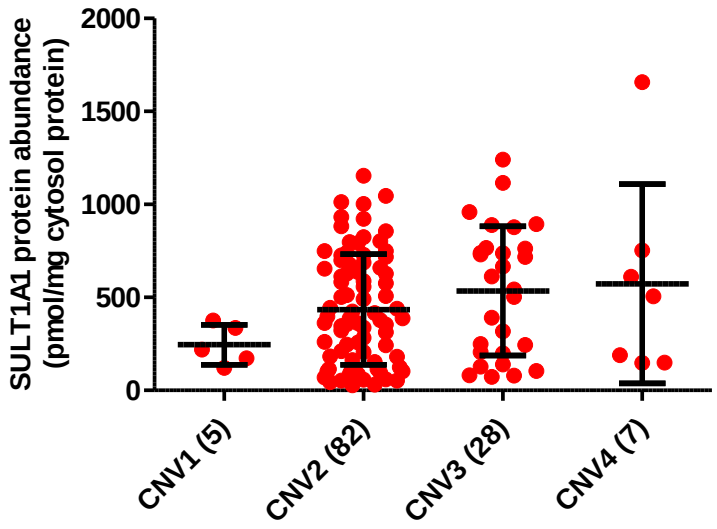

Supplemental Fig. 4. Association of SULT1A1 copy number variation (CNV) with hepatic SULT1A1 protein abundance in pediatric samples. Statistical analysis was performed using Kruskal-Wallis test followed by Dunn's multiple comparison test. The number of samples in each CNV is indicated in parentheses on the x-axis.

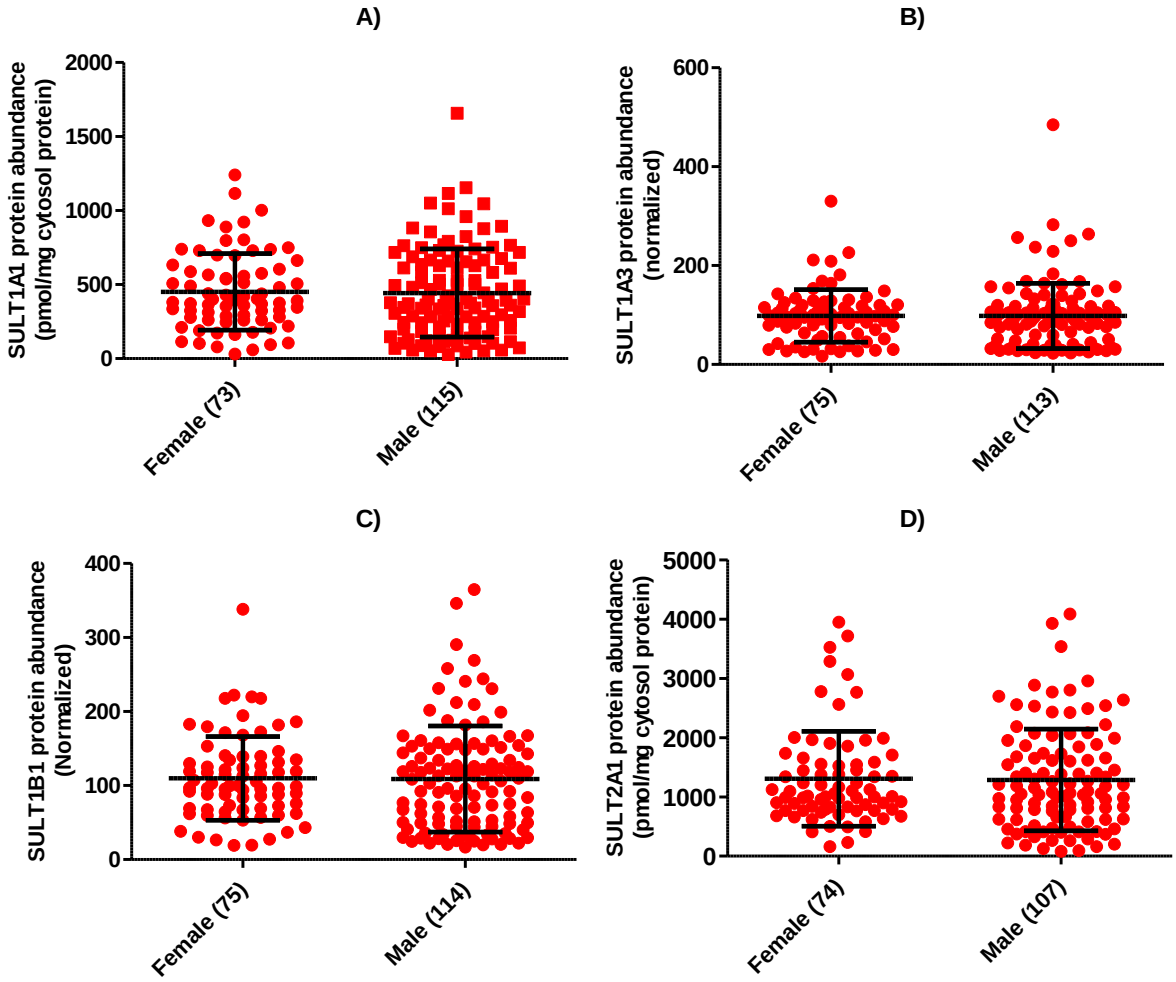

Supplemental Fig. 5. Association of sex with protein abundance of hepatic SULT1A1 (A), SULT1A3 (B), SULT1B1 (C) and SULT2A1 (D). Statistical analysis was performed using Mann-Whitney test. The number of samples in each sex category is indicated in parentheses on the x-axis.

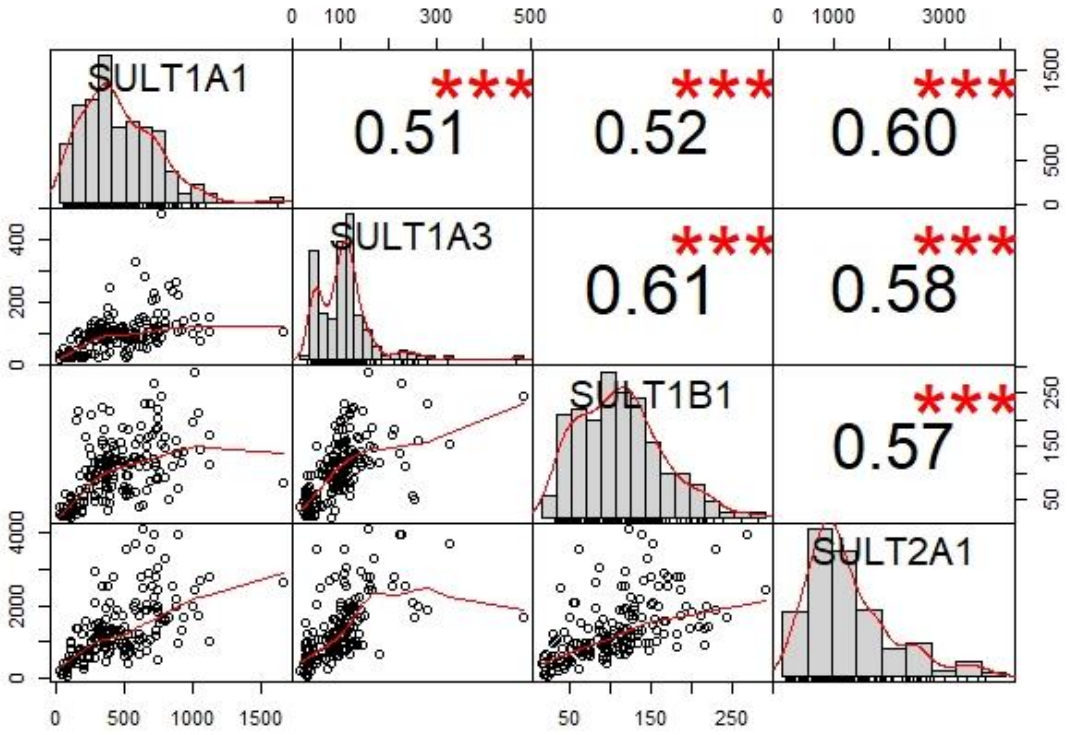

Supplemental Fig. 6. Correlation between protein abundances of SULT proteins. *** represents p-values <0.001.

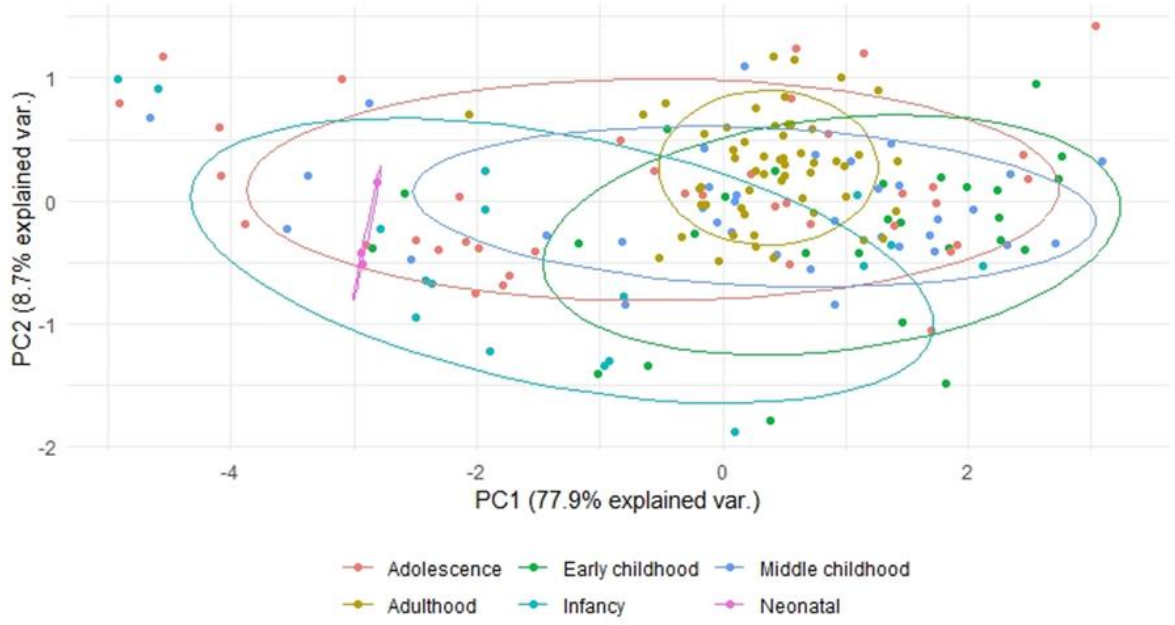

Supplemental Fig. 7. Principal component analysis (PCA) of SULT protein abundance across various age groups. The plot shows absence of cluster on lower left side indicating robustness of sample handling and storage. Also, evidently the adult data for all SULT proteins have less variability than in pediatric populations of different ages.

Supplemental Table

Supplemental Table 1. LC gradient program for analysis of surrogate peptides of SULTs.

Time (minutes)	Flow rate (mL/minute)	Mobile phase A-Water with 0.1% formic acid (%)	Mobile phase B-Acetonitrile with 0.1% formic acid (%)
0.0	0.3	97	3
4	0.3	97	3
8	0.3	87	13
18	0.3	70	30
20.5	0.3	65	35
21.1	0.3	40	60
23.1	0.3	20	80
23.2	0.3	97	3
27	0.3	97	3

Supplemental Table 2. Optimized mass instrument parameters for analysis of surrogate peptides of SULTs enzyme and bovine serum albumin (BSA).

	Protein/peptide sequences	Light/ Heavy	Parent ion (m/z)	Product ion (m/z)	DP* (V)	CE# (eV)
SULT1A1	VHPEPGTWDSFLEK	Light	547.94	237.14	71	27
			821.4	237.14	91	37
			821.4	703.34	91	37
		Heavy	550.61	237.14	71	27
			825.41	237.14	91	37
	ILEFVGR	Light	417.25	607.32	80	23
			417.25	478.28	80	23
			417.25	356.21	80	23
		Heavy	422.25	617.32	80	23
			422.25	488.28	80	23
SULT2A1	NHFTVAQAEDFDK	Light	761.35	399.18	87	33
			761.35	1270.6	87	33
			761.35	1123.53	87	33
		Heavy	765.36	399.18	87	33
			765.36	1131.54	87	33
	TLEPEELNLILK	Light	706.41	344.18	83	33
			706.41	1068.63	83	33
			706.41	260.2	83	33
		Heavy	710.41	344.18	83	33
			710.41	1076.64	83	33
SULT1B1	NYFTVAQNEK	Light	607.3	278.11	75	28
			607.3	425.18	75	28
			607.3	789.41	75	28
		Heavy	611.3	278.11	75	28
			611.3	425.18	75	28
SULT1A3	AHPEPGTWDSFLEK	Light	538.59	209.1	70	24
			538.59	345.66	70	24
			538.59	690.32	70	24
			538.59	738.37	70	24
			538.59	924.45	70	24
		Heavy	541.26	209.1	70	24
			541.26	746.38	70	24
BSA	LVNELTEFAK	Light	582.32	595.31	70	31
			582.32	951.48	70	31
			582.32	218.15	70	31
		Heavy	586.33	603.32	70	31
			586.33	959.49	70	31
			586.33	226.16	70	31

*DP, declustering potential; and #CE, collision energy.

Supplemental Table 3. Drug and system specific input parameters for acetaminophen model development.

Properties	Parameters	Values/models
Physiochemical	Molecular weight (g/mol)	151.17[a]
	LogP	0.51[b]
	pK_a	9.46[b]
	Solubility (mg/mL) (pH=8.94)	13.65[a]
	B:P	1.58[b]
	fu_p	0.82[b]
Absorption	Absorption model	ACAT[c]
	P_{eff} (10^{-4} cm/sec)	12[a]
	Diffusion coefficient ($10^{-5}cm^2$/sec)	1.11[c]
	Dissolution model	Johnson[c]
	Particle size distribution	Log-normal[c]
	Particle radius (μm)	25[c]
	Particle density (g/mL)	1.2[c]
	Dose volume (mL)	250[c]
	Precipitation model	First order[c]
	Precipitation time (sec)	900[c]
	Paracellular model	Zhimin[c]
Distribution	Distribution Model	Full PBPK-Lukacova method[c]
	V_{ss} (L/kg)	0.99[d]
Elimination	CL_{IV} (L/h)	19.7[b]
	$f_{CL,renal}$ (CL_R in L/h)	0.057[e] (1.12)[f]
	$f_{CL,metabolism,H}$ (CL_H in L/h)	0.943[e] (18.58)[g]
Metabolic clearance	$CLu_{int,H}$ in L/h	26.32[h]
	$f_{m,UGT}$ ($CLu_{int,UGT}$ in L/h)	0.54[e] (15.07)[i]
	$f_{m,SULT}$ ($CLu_{int,SULT}$ in L/h)	0.31[e] (8.65)[i]
	$f_{m,CYP}$ ($CLu_{int,CYP}$ in L/h)	0.093[e] (2.60)[i]
Fraction unbound	fu_{mic}	1[b,c]
Adult enzyme expression (mg enzyme/g tissue)	UGT1A1	0.052[c]
	UGT1A9	0.050[c]
	UGT2B15	0.265[c]
	SULT1A1	0.257[c]
	SULT1A3	0.038[c]

	SULT1E1		0.027[c]	
	SULT2A1		0.155[c]	
	CYP1A2		0.115[c]	
	CYP2C9		0.154[c]	
	CYP2C19		0.030[c]	
	CYP2D6		0.017[c]	
	CYP2E1		0.132[c]	
	CYP3A4		0.242[c]	
UGTs	**f_{m,UGT_j}** (% contribution of UGT)	**K_m (µM)**	**V_{max} (pmol/min/mg microsomal protein)[j]**	**CLu_{int} (L/h)[i]**
UGT1A1	0.162[k] (30)[b]	5500[l]	6661.13	4.52
UGT1A9	0.162[k] (30)[b]	9200[l]	11142.25	4.52
UGT2B15	0.216[k] (40)[b]	23000[l]	37140.84	6.03
SULTs	**$f_{m,SULT_j}$** (% contribution of SULT)	**K_m (µM)**	**V_{max} (pmol/min/mg cytosolic protein)[j]**	**CLu_{int} (L/h)[i]**
SULT1A1	0.176[k] (57)[m]	2400[n]	1498.79	4.91
SULT1A3	0.042[k] (13)[m]	1500[n]	221.70	1.16
SULT1E1	0.024[k] (8)[m]	1900[n]	159.25	0.66
SULT2A1	0.06[k] (22)[m]	3700[n]	905.52	1.92
CYPs	**f_{m,CYP_j}** (% contribution of CYP)	**K_m (µM)**	**V_{max} (pmol/min/mg microsomal protein)[j]**	**CLu_{int} (L/h)[i]**
CYP1A2	0.021[k] (22)[o]	220[p]	33.65	0.57
CYP2C9	0.002[k] (2)[o]	660[p]	9.18	0.052
CYP2C19	0.002[k] (2)[o]	2000[p]	27.81	0.052
CYP2D6	0.002[k] (2)[o]	440[p]	6.12	0.052
CYP2E1	0.003[k] (3)[o]	4020[q]	83.85	0.078
CYP3A4	0.064[k] (69)[o]	130[p]	62.37	1.791

Abbreviations: LogP, partition coefficient; pKa, dissociation constant; B:P, blood to plasma concentration ratio; fu_p, unbound fraction in the plasma, fu_{mic}, unbound fraction in the microsomes, P_{eff}, effective permeability; V_{ss}, volume of distribution at steady state; CL_{IV}, intravenous plasma clearance; CL_H, hepatic plasma clearance, CL_R, renal plasma clearance; $f_{CL,renal}$, fraction of drug cleared unchanged renally; $f_{CL,metabolism,H}$, fraction of drug cleared through hepatic metabolism (calculated as 1- $f_{CL,renal}$) (Bohnert et al., 2016) and $f_{m,DME}$, fraction of drug metabolized by a drug metabolizing enzyme. For method/references, details are as follows: [a](Villiger et al., 2016); [b](Jiang et al.,

2013); [c]Default value in GastroPlus; [d]Optimized according to literature reported (Jiang et al., 2013) value in adult by adjusting LogP value (1.33) with default tissue:plasma partition coefficient (Kp) methods (Lukacova for perfusion-limited and Poulin & Theil extracellular for permeability-limited tissues) using PBPKPlus module of GastroPlus. Similar approach was used for V_{ss} calculation in children; [e](Critchley et al., 1986); [f]$CL_R = f_{CL,renal} \times CL_{IV}$; [g]$CL_H = f_{CL,metabolism,H} \times CL_{IV}$ or $CL_{IV} - CL_R$; [h]Calculated using eq. 2, as described in the text; [i]Calculated using eq. 3; [j]Calculated using eq. 5, as described in the text; [k]$f_{m,DME_j} = (f_{m,DME} \times$ % contribution of DME)/100; [l](Laine et al., 2009); [m]contribution values (%) of SULT isoforms were calculated from eq. 4, as described in the Supplemental Methodology; [n](Adjei et al., 2008); [o]contribution values (%) of CYP isoforms were calculated from eq. 2, as described in the Supplemental Methodology; [p](Laine et al., 2009), and [q](Laine et al., 2009).

Supplemental Table 4. Input parameters for glucuronide metabolite PBPK model.

Properties	Parameters	Values/models
Physiochemical	Molecular weight (g/mol)	327.29[a]
	LogP	-1.16[a]
	pK_a	11.34 (acid)[a] 3.92 (acid)[a]
	Solubility factor	8.23[a]
	Solubility (mg/mL) (pH=2.43)	38.43[a]
	B:P	0.67[a]
	fu_p	0.92[b]
	fu_{mic}	1[a]
Absorption	Absorption model	ACAT[a]
	P_{eff} (10^{-4} cm/ sec)	0.38[a]
	Diffusion coefficient ($10^{-5}cm^2$/sec)	0.77[a]
	Dissolution model	Johnson[a]
	Particle size distribution	Log-normal[a]
	Particle radius (µm)	25[a]
	Particle density (g/mL)	1.2[a]
	Dose volume (mL)	250[a]
	Precipitation model	First order[a]
	Precipitation time (sec)	900[a]
	Paracellular model	Zhimin[a]
Distribution	Distribution model	Full PBPK-Lucakova method[a]
	V_{ss} (L)	20.797[a]
Elimination	CL_H (L/h)	0[a]
	CL_R (L/h)	35[c]

For method/references, details are as follows: [a]Determined using ADMET Predictor v9.0.; [b](Morris and Levy, 1984), and [c]Optimized to achieve formation-rate limited kinetics as described in the text.

Supplemental Table 5. Input parameters for sulfate metabolite PBPK model.

Properties	Parameters	Values/models
Physiochemical	Molecular weight (g/mol)	231.23[a]
	LogP	-0.0973[a]
	pK_a	11.42 (acid)[a] 0.21 (acid)[a]
	Solubility factor	175.8[a]
	Solubility (mg/mL) (pH=1.72)	4.54[a]
	B:P	0.77[a]
	fu_p	0.46[b]
	fu_{mic}	1[a]
Absorption	Absorption model	ACAT[a]
	P_{eff} (10^{-4} cm/sec)	2.89[a]
	Diffusion coefficient ($10^{-5}cm^2$/sec)	0.93[a]
	Dissolution model	Johnson[a]
	Particle size distribution	Log-normal[a]
	Particle radius (µm)	25[a]
	Particle density (g/mL)	1.2[a]
	Dose volume (mL)	250[a]
	Precipitation model	First order[a]
	Precipitation time (sec)	900[a]
	Paracellular model	Zhimin[a]
Distribution	Distribution model	Full PBPK-Lucakova method[a]
	V_{ss} (L)	15.399[a]
Elimination	CL_H (L/h)	0[a]
	CL_R (L/h)	14.291[c]

For method/references, details are as follows: [a]Determined using ADMET Predictor v9.0.; [b](Morris and Levy, 1984), and [c]Optimized to achieve formation-rate limited kinetics as described in the text.

Supplemental Table 6. Scaling factors (SF) for mean, lower and higher 95% CI UGT and SULT abundances for individual age groups and various SF_{MPPGL} values.

Age groups (range)	SF_{UGT1A1}	SF_{UGT1A9}	$SF_{UGT2B15}$	$SF_{SULT1A1}$	$SF_{SULT1A3}$	$SF_{SULT1E1}$	$SF_{SULT2A1}$	SF_{MPPGL}
Mean								
Neonatal[#] (0 to 27 days)	0.12	0.03	0.39	0.24	0.47	2.66	0.38	0.64
Infancy[#] (28 to 364 days)	0.43	0.24	0.60	0.80	0.76	1.64	1.11	0.65
Infancy* (29 to <2 years)	0.39	0.24	0.54	0.97	0.79	1.56	1.15	0.65
Toddler/early childhood[#] (1 to <6 years)	0.69	0.38	0.64	1.57	1.14	1.20	1.63	0.70
Middle childhood[#] (6 to <12 years)	0.64	0.43	0.67	1.25	0.99	1.15	1.30	0.75
Children* (2 to <12 years)	0.69	0.40	0.67	1.36	1.06	1.20	1.46	0.72
Adolescence* (12 to 16 years)	0.46	0.38	0.81	0.90	0.86	1.15	0.89	0.92
Adolescence[#] (12 to 18 years)	0.46	0.39	0.83	0.98	0.88	1.00	0.97	0.92
Adulthood[#] (>18 years)	1.00	1.00	1.00	1.00	1.00	1.00	1.00	1.00
Lower 95% CI								
Neonatal[#] (0 to 27 days)	0.05	0.02	0.005	0.12	0.11	1.23	0.10	0.64
Infancy* (28 to 364 days)	0.28	0.15	0.47	0.47	0.38	1.42	0.66	0.65
Infancy* (29 to <2 years)	0.27	0.16	0.42	0.62	0.47	1.36	0.75	0.65
Toddler/early childhood[#] (1 to <6 years)	0.47	0.29	0.51	1.26	0.86	0.94	1.29	0.70
Middle childhood[#] (6 to <12 years)	0.46	0.33	0.57	1.01	0.81	0.87	1.01	0.75

Children* (2 to <12 years)	0.55	0.34	0.60	1.17	0.90	0.99	1.23	0.72
Adolescence* (12 to 16 years)	0.32	0.29	0.72	0.64	0.55	0.64	0.64	0.92
Adolescence# (12 to 18 years)	0.35	0.32	0.74	0.76	0.65	0.70	0.76	0.92
Adulthood# (> 18 years)	0.79	0.86	0.84	0.89	0.95	0.70	0.91	1.00
Higher 95% CI								
Neonatal# (0 to 27 days)	0.19	0.04	0.77	0.35	0.83	4.10	0.65	0.64
Infancy# (28 to 364 days)	0.57	0.33	0.73	1.12	1.14	1.87	1.57	0.65
Infancy* (29 to <2 years)	0.51	0.31	0.66	1.32	1.11	1.77	1.55	0.65
Toddler/early childhood# (1 to <6 years)	0.92	0.46	0.76	1.89	1.41	1.46	1.98	0.70
Middle childhood# (6 to <12 years)	0.81	0.53	0.78	1.48	1.17	1.42	1.60	0.75
Children* (2 to <12 years)	0.83	0.46	0.75	1.56	1.22	1.41	1.69	0.72
Adolescence* (12 to 16 years)	0.60	0.47	0.90	1.15	1.17	1.67	1.14	0.92
Adolescence# (12 to 18 years)	0.57	0.46	0.91	1.20	1.12	1.30	1.17	0.92
Adulthood# (>18 years)	1.20	1.14	1.16	1.11	1.05	1.30	1.09	1.00

#Age classification based on NICHD/NIH; *Age classification based on the USFDA.

Supplemental Table 7. Key ontogeny parameters describing abundance-based developmental trajectories of SULT enzymes.

		A_{birth}	A_{max}	Age_{50}	h
SULT1A3	Mean	85.26	96.83	0.9094	166.5
	SE	12.52	4.78	0.1198	4767
	95% CI	60.73 to 109.8	87.46 to 106.2	0.6746 to 1.144	0.0 to 9509
SULT1B1	Mean	37.75	116.8	0.9092	166
	SE	4.868	4.899	0.01347	656.6
	95% CI	28.21 to 47.29	107.2 to 126.4	0.8828 to 0.9356	0.0 to 1453

Abbreviations: A_{birth}, enzyme abundance at birth; A_{max}, maximum average enzyme abundance; Age_{50}, age in years at which 50% enzyme abundance is reached; h, Hill coefficient; SE, standard error; and CI, confidence intervals.

Supplemental Table 8. Multiple linear regression analysis of predictors associated with interindividual variability of SULTs protein abundance.

Dependent variable	Independent variable	Effect size β (Coefficient)	Standard error (SE)	t value	p-value
SULT1A1 abundance	(Intercept)	400.405	203.247	1.970	0.050430
	Adulthood	-7.621	90.141	-0.085	0.932718
	Toddler/early childhood	211.573	59.108	3.579	0.000447***
	Infancy	22.004	73.468	0.300	0.764910
	Middle childhood	64.842	55.113	1.177	0.240997
	Neonatal	-207.744	127.341	-1.631	0.104625
	Female	347.756	177.3	1.961	0.051437
	Male	348.202	176.668	1.971	0.050326
	African American	-333.657	63.832	-5.227	4.92E-07***
	Caucasian	-286.810	49.476	-5.797	3.13E-08***
	CNV1	-353.545	142.155	-2.487	0.013829*
	CNV2	-152.472	96.044	-1.588	0.114220
	CNV3	-82.061	101.312	-0.810	0.419063
	CNV4	-77.626	131.343	-0.591	0.555280
	rs9282861A/A	-78.8	111.475	-0.707	0.480588
	rs9282861A/G	-69.266	88.255	-0.785	0.433621
	rs9282861G/G	-37.338	92.542	-0.403	0.687098
SULT1A3 abundance	(Intercept)	64.56	40.85	1.58	0.1158
	Adulthood	22.37	11.64	1.922	0.0562
	Toddler/early childhood	24.11	13.34	1.807	0.0724
	Infancy	9.89	16.56	0.597	0.5512
	Middle childhood	8.36	12.41	0.674	0.5013
	Neonatal	-15.44	29.48	-0.524	0.6011
	Female	61.64	40.86	1.509	0.1332
	Male	64.69	40.66	1.591	0.1134
	African American	-81.98	14.49	-5.659	5.91E-08***
	Caucasian	-47.52	11.17	-4.256	3.35E-05***
SULT1B1 abundance	(Intercept)	90.7278	41.2704	2.198	0.0292*
	Adulthood	7.8164	18.7774	0.416	0.6777
	Toddler/early childhood	13.7968	13.3653	1.032	0.3034
	Infancy	-41.5382	16.8152	-2.470	0.0145*
	Middle childhood	-0.7525	12.6489	-0.059	0.9526
	Neonatal	-58.3861	34.293	-1.703	0.0904
	Female	69.2022	41.3422	1.674	0.0959
	Male	72.32	41.1171	1.759	0.0803
	African American	-90.0892	14.8453	-6.069	7.78E-09***

	Caucasian	-66.5892	11.4187	-5.832	2.59E-08***
	rs11731028A/A	-19.3662	68.0525	-0.285	0.7763
	rs11731028A/G	-13.3737	63.615	-0.21	0.8337
	rs11731028G/G	-11.6572	59.1593	-0.197	0.844
	rs1604741C/C	45.0067	63.9997	0.703	0.4828
	rs1604741C/T	15.8329	59.8326	0.265	0.7916
	rs1604741T/T	17.3327	59.0353	0.294	0.7694
SULT2A1 abundance	(Intercept)	465.97	547.23	0.852	0.39569
	Adulthood	-40.45	261.52	-0.155	0.87728
	Toddler/early childhood	752.07	182.27	4.126	5.77E-05***
	Infancy	417.36	224.63	1.858	0.06490
	Middle childhood	316.38	171.99	1.84	0.06758
	Neonatal	-368.16	395.61	-0.931	0.35337
	Female	1109.81	547.39	2.027	0.04418*
	Male	1090.45	545.08	2.001	0.04703*
	African American	-934.13	199.34	-4.686	5.68E-06***
	Caucasian	-611.08	156.03	-3.916	0.00013***
	rs296365C/C	291.32	250.73	1.162	0.24691
	rs296365C/G	149.28	278.3	0.536	0.59239
	rs296365G/G	72.8	492.93	0.148	0.88276

*, ** and *** represents p-values <0.05, <0.01 and <0.001, respectively.

Supplemental Table 9. Summary of Jonckheere-Terpstra (JT) test results (alternative hypothesis: two-sided).

	Covariate	JT Statistic	p-value	p-value (with nperm = 1000)
SULT1A1 abundance	*Age groups* (neonatal-infancy-toddler/early childhood-middle childhood-adolescence-adulthood)	6784	0.5249	0.528
	rs982861 (AA-AG-GG)	550	0.4536	NA
	CNV (1-2-3-4)	2099	0.03078*	0.036*
SULT1A3 abundance	*Age groups* (neonatal-infancy-toddler/early childhood-middle childhood-adolescence-adulthood)	7785	0.08674	0.092
SULT1B1 abundance	*Age groups* (neonatal-infancy-toddler/early childhood-middle childhood-adolescence-adulthood)	8375	0.00332*	0.006*
	rs11569731 (CT-TT)	256	0.08281	0.094
	rs11249460 (CC-CT-TT)	342.5	0.03348*	0.03*
	rs11731028 (AA-AG-GG)	440.5	0.1403	0.142
	rs1604741 (CC-CT-TT)	423.5	0.1257	0.102
SULT2A1 abundance	*Age groups* (neonatal-infancy-toddler/early childhood-middle childhood-adolescence-adulthood)	3856	0.7663	0.744
	rs296365 (CC-CG-GG)	282	0.065	0.058

*Significant associations (p-value < 0.05).

Supplemental Table 10. Predicted exposure parameters for intravenous administration of acetaminophen according to modified dosing regimen by the USFDA in neonates and infants.

Clinical PK studies	Details (mean age)	Predicted (P) $AUC_{0\text{-}6\ h}$ (μg·h/mL)	Results	Observed (O) $AUC_{0\text{-}6\ h}$ (μg·h/mL)	P/O ratio
Acetaminophen injection	Neonatal (14 days)	34.18	Comparable with children	38	0.90
Acetaminophen injection	Infancy (1 year)	26.58	Comparable with children	38	0.70
Acetaminophen injection (OFIRMEV)	Neonatal (14 days)	57.14	Comparable with adult	43	1.33

Acetaminophen injection for intravenous use, 7.5 mg/kg dose (CDER, 2010), and acetaminophen injection (OFIRMEV), 12.5 mg/kg dose (CDER, 2015).

References

Adjei AA, Gaedigk A, Simon SD, Weinshilboum RM, and Leeder JS (2008) Interindividual variability in acetaminophen sulfation by human fetal liver: implications for pharmacogenetic investigations of drug-induced birth defects. *Birth Defects Res A Clin Mol Teratol* **82:**155-165.

Bhatt DK, Gaedigk A, Pearce RE, Leeder JS, and Prasad B (2017) Age-dependent protein abundance of cytosolic alcohol and aldehyde dehydrogenases in human liver. *Drug Metab Dispos* **45:**1044-1048.

Bohnert T, Patel A, Templeton I, Chen Y, Lu C, Lai G, Leung L, Tse S, Einolf HJ, and Wang Y-H (2016) Evaluation of a new molecular entity as a victim of metabolic drug-drug interactions-an industry perspective. *Drug Metab Dispos* **44:**1399-1423.

CDER (2010) Application number 022450. Clinical Pharmacology and Biopharmaceutics Review(s) https://www.accessdata.fda.gov/drugsatfda_docs/nda/2010/022450Orig1s000ClinPharmR.pdf.

CDER (2015) Application number 204767. Printed Labeling https://www.accessdata.fda.gov/drugsatfda_docs/nda/2015/204767Orig1s000TOC.cfm.

Chen W, Koenigs LL, Thompson SJ, Peter RM, Rettie AE, Trager WF, and Nelson SD (1998) Oxidation of acetaminophen to its toxic quinone imine and nontoxic catechol metabolites by baculovirus-expressed and purified human cytochromes P450 2E1 and 2A6. *Chem Res Toxicol* **11:**295-301.

Court MH, Duan SX, von Moltke LL, Greenblatt DJ, Patten CJ, Miners JO, and Mackenzie PI (2001) Interindividual variability in acetaminophen glucuronidation by human liver microsomes: identification of relevant acetaminophen UDP-glucuronosyltransferase isoforms. *J Pharmacol Exp Ther* **299:**998-1006.

Critchley J, Nimmo G, Gregson C, Woolhouse N, and Prescott L (1986) Inter-subject and ethnic differences in paracetamol metabolism. *Br J Clin Pharmacol* **22:**649-657.

De Morais SM, Uetrecht JP, and Wells PG (1992) Decreased glucuronidation and increased bioactivation of acetaminophen in Gilbert's syndrome. *Gastroenterology* **102:**577-586.

Jiang XL, Zhao P, Barrett J, Lesko L, and Schmidt S (2013) Application of physiologically based pharmacokinetic modeling to predict acetaminophen metabolism and pharmacokinetics in children. *CPT Pharmacometrics Syst Pharmacol* **2:**1-9.

Laine J, Auriola S, Pasanen M, and Juvonen R (2009) Acetaminophen bioactivation by human cytochrome P450 enzymes and animal microsomes. *Xenobiotica* **39:**11-21.

Miners JO, Bowalgaha K, Elliot DJ, Baranczewski P, and Knights KM (2011) Characterization of niflumic acid as a selective inhibitor of human liver microsomal UDP-glucuronosyltransferase 1A9: application to the reaction phenotyping of acetaminophen glucuronidation. *Drug Metab Dispos* **39:**644-652.

Morris ME and Levy G (1984) Renal clearance and serum protein binding of acetaminophen and its major conjugates in humans. *J Pharm Sci* **73:**1038-1041.

Mutlib AE, Goosen TC, Bauman JN, Williams JA, Kulkarni S, and Kostrubsky S (2006) Kinetics of acetaminophen glucuronidation by UDP-glucuronosyltransferases 1A1, 1A6, 1A9 and 2B15. Potential implications in acetaminophen-induced hepatotoxicity. *Chem Res Toxicol* **19:**701-709.

Navarro SL, Chen Y, Li L, Li SS, Chang J-L, Schwarz Y, King IB, Potter JD, Bigler J, and Lampe JW (2011) UGT1A6 and UGT2B15 polymorphisms and acetaminophen conjugation in response to a randomized, controlled diet of select fruits and vegetables. *Drug Metab Dispos* **39:**1650-1657.

Villiger A, Stillhart C, Parrott N, and Kuentz M (2016) Using physiologically based pharmacokinetic (PBPK) modelling to gain insights into the effect of physiological factors on oral absorption in paediatric populations. *AAPS J* **18:**933-947.